Structural and Mechanistic Features of Protein O Glycosylation Linked to CD8+ T-Cell Apoptosis[∇][†]

Steven J. Van Dyken, Ryan S. Green, and Jamey D. Marth*

Howard Hughes Medical Institute and Department of Cellular and Molecular Medicine, University of California, San Diego, 9500 Gilman Drive, La Jolla, California 92093-0625

CD8+ T-cell apoptosis is essential for the contraction phase of the immune response, yet the initiating signals and precise pathways involved are unresolved. The ST3Gal-I sialyltransferase is a candidate mechanistic component and catalyzes sialic acid addition to core 1 O-glycans during protein O glycosylation. ST3Gal-I inactivation or enzymatic removal of its product renders CD8+ T cells, but not CD4+ T cells, susceptible to apoptosis by differential cross-linking of O-glycoproteins in the absence of interleukin-2 and T-cell receptor (TCR) signaling. This results in caspase activation, DNA fragmentation, and phosphatidylserine externalization prior to cell death. We further show that ST3Gal-I function is regulated by a posttranscriptional mechanism operating distal to Golgi core 2 O glycosylation and is invariably linked to CD8+ T-cell contraction following viral (lymphocytic choriomeningitis virus) infection and bacterial (staphylococcal enterotoxin B) antigen immunization. The mechanism does not involve the ST3Gal-I substrate CD43 or core 2 O-glycan induction and overcomes the ability of Bcl-2 to inhibit the contraction phase in vivo. Loss of ST3Gal-I function further reduces Bim-deficient CD8+ T-cell accumulation without diminishing apoptotic sensitivity. We propose that an endogenous lectin activates an apoptotic pathway constructed in CD8+ T cells following TCR stimulation and enables contraction upon attenuation of immune signaling.

Cellular homeostasis within the adaptive immune system reflects a balance between the production and turnover of lymphocytes. The burst of CD8+ T-cell numbers that occurs following an immune stimulus precedes an almost equally large reduction in cellularity to near preimmune levels during the contraction phase and resolution of the immune response when antigen abundance has been substantially reduced. This post-immune contraction in CD8+ T-cell number is linked to cell death by apoptosis; however, the mechanism(s) controlling this process remain to be elucidated (15, 19). There is reason to believe that different types of lymphocytes undergo apoptosis by different mechanisms, and recent studies have found that this includes the Th1 and Th2 CD4+ T-cell subtypes (11, 52, 53).

Current concepts of CD8+ T-cell apoptosis include the extrinsic or death receptor-mediated pathway and the intrinsic or mitochondrial death pathway (57). The extrinsic pathway is thought to depend on extracellular receptor-ligand binding to directly activate a death signal, which has been described as mediated by members of the tumor necrosis factor receptor family. Some studies have implicated a role for Fas and tumor necrosis factor signaling (28). These ligand-receptor systems have also been found to induce nonapoptotic signals, such as costimulation, depending on culture conditions (54). Importantly, mice deficient in these receptors and their ligands ex- hibit normal CD8+ T-cell apoptotic contraction following immune stimulation in vivo (21, 30, 39, 45, 49, 50).

In contrast, the intrinsic pathway of CD8+ T-cell apoptosis is thought to depend upon signals arising in a cell-autonomous manner which tip the balance of intracellular pro- and anti-apoptotic proteins that include the Bcl-2 family, which regulate mitochondrial membrane permeability (17, 33). Indeed, T cells in mice overexpressing Bcl-2 are more resistant to apoptotic death and display prolonged survival in vivo in response to immunization with the superantigen *Staphylococcus aureus* enterotoxin B (SEB) (21, 56). The proapoptotic Bcl-2 family member Bim also appears to be a key intracellular factor regulating the death of mature T cells. Interestingly, in contrast to Bcl-2 overexpression, Bim-deficient mice accumulate peripheral T and B lymphocytes in vivo, and their thymocytes are resistant to apoptotic stimuli in vitro (5). Peripheral CD4+ and CD8+ T cells lacking Bim display prolonged survival in response to SEB immunization as well as following infection with herpes simplex virus (21, 45).

Mediators of CD8+ T-cell apoptosis include, but are not limited to, perforin, gamma interferon, granzyme B, and reactive oxygen species. Nevertheless, perforin-deficient mice exhibit normal contraction of CD8+ T cells in response to an attenuated strain of *Listeria monocytogenes*, while chronic lymphocytic choriomeningitis virus (LCMV) infection in these mice leads to accumulation of virus-specific CD8+ T cells (2, 34, 63). Gamma interferon-deficient mice display delayed T-cell contraction after bacterial and viral infection, which could be due to hyperproliferation with failure to effectively clear pathogen (2, 4, 31, 44). Gamma interferon-dependent inflammation early in the immune response does appear to regulate the initial expansion phase that makes CD8+ T-cell contraction possible (3). Apoptosis may also be mediated by reactive
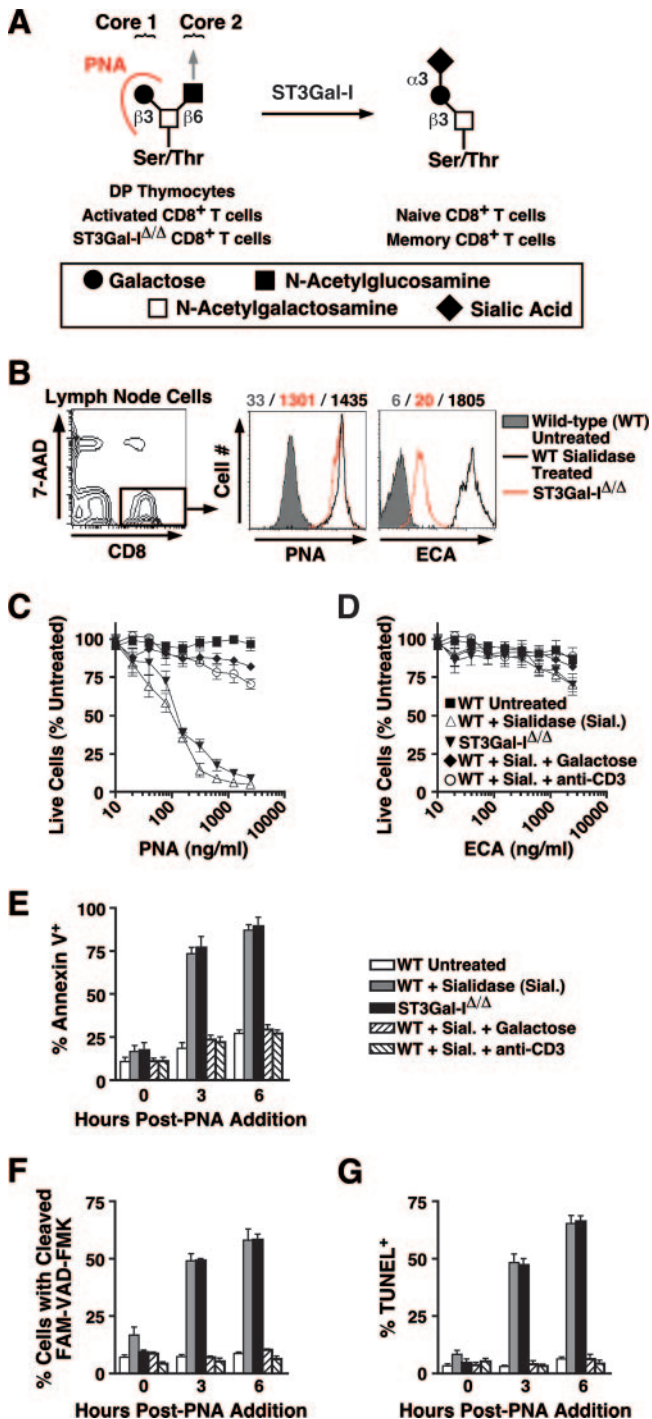
FIG. 1. O-glycan structures and sialidase treatment sensitize wild-type CD8$^+$ T cells to apoptotic death in vitro. (A) ST3Gal-I-dependent sialylation of the core 1 O-glycan Galβ1-3GalNAc-Ser/Thr can be monitored by differential PNA binding. Immature CD4/CD8 double-positive thymocytes and activated peripheral CD8$^+$ T cells, as well as ST3Gal-I$^{\Delta/\Delta}$ CD8$^+$ T cells, express the unsialylated core 1 O-glycan Galβ1-3GalNAc-Ser/Thr, which is the ligand for PNA lectin, whereas this structure is predominantly sialylated among wild-type naive and memory cells. The position of the core 2 branch and possible extension is indicated by an arrow. (B) Flow cytometric analysis of PNA and ECA ligand levels among live (7-AAD$^-$) wild-type CD8$^+$ T cells treated with *Vibrio cholerae* sialidase, along with nontreated ST3Gal-I$^{\Delta/\Delta}$ CD8$^+$ T cells. Mean fluorescence intensity values are indicated by

oxygen species, as reduction using the superoxide dismutase mimetic (MnTBAP) protected T cells from death in vitro (20). In addition, the role of serine protease inhibitor 6 has been recently described in protecting against CD8$^+$ T-cell death caused by granzyme B-mediated breakdown of intracellular cytotoxic granules (62).

It is evident that the apoptotic death of postactivated CD8$^+$ T cells can be modulated by multiple factors, although the potential remains for the existence of an apoptotic signaling network that is enabled and perhaps activated by one type or a few types of cell surface molecules. In this case, the attributes of such a cell surface molecule or modification might include its induction or activation at the cell surface following immune stimulation and perhaps at later stages of activation. A second expectation would be that the function of such a molecule among naive CD8$^+$ T cells should induce caspase-dependent apoptotic signals that result in a decrease in peripheral CD8$^+$ T-cell homeostasis in the absence of immune stimulation.

A candidate cell surface alteration that fits this profile of an apoptotic regulator operating in post-immune CD8$^+$ T-cell contraction has been identified as a change in protein O glycosylation involving the ST3Gal-I sialyltransferase (48). A significant reduction in the sialic acid linkage on core 1 O-glycans indicative of ST3Gal-I deficiency marks activated and effector CD8$^+$ T cells that are destined either for apoptosis or differentiation into memory CD8$^+$ T cells, the latter of which appear with increased levels of sialylated core 1 O-glycans due to ST3Gal-I activity (14, 48). The unsialylated core 1 O-glycan structure is detected by the peanut agglutinin (PNA) lectin, and ST3Gal-I deficiency is also permissive for an increase of 1B11 antibody-reactive core 2 O-glycans (Fig. 1A). When this postactivated cell surface O glycotype is produced on naive CD8$^+$ T cells, apoptosis occurs by caspase-dependent mechanisms that vastly reduce the pool of peripheral naive CD8$^+$ T cells (48).

We have investigated the structure-function relationship of these O-glycan changes as they normally occur in vivo and have characterized this form of O-glycoprotein regulation in modulating CD8$^+$ T-cell apoptosis among primary CD8$^+$ T cells. By constitutively expressing ST3Gal-I, we have sought to inhibit this apoptotic signaling, and by breeding ST3Gal-I deficiency into mice bearing antiapoptotic phenotypes afforded by altered Bcl-2 and Bim expression, we have discerned novel mechanistic attributes regarding how altered protein O glycosylation enables CD8$^+$ T-cell apoptosis in the contraction phase of the immune response.

the corresponding colored numbers. These cells were subsequently cultured for 24 h with PNA (C) or ECA (D) at the indicated concentrations. Cell counts are presented as percentages of live CD8$^+$ T cells compared to control cultures not treated with sialidase or lectin. The percentage of cells among the live (7-AAD$^-$) cell population in culture 0, 3, and 6 h after addition of 1,000 ng/ml PNA positive for annexin V (E), active caspases, assessed by 6-carboxyfluorescein (FAM)-VAD-FMK cleavage (F), and DNA fragmentation, assessed by terminal deoxynucleotidyltransferase-mediated dUTP-biotin nick end labeling (TUNEL) assay was measured by flow cytometry (G). Data are presented as means ± standard errors of the means (n = 4).

MATERIALS AND METHODS

Mice. The ST3Gal-I transgene used in generating ST3Gal-I transgenic (ST3Gal-I^{Tg}) mice was constructed by inserting the 2-kb EcoRI fragment of human ST3Gal-I cDNA (24) (GenBank accession no. L29555) into the VA human CD2 (hCD2) minigene cassette (64). The resulting 13.2-kb transgene (liberated from plasmid with KpnI and XbaI) was microinjected into the pronuclei of zygotes from hybrid strain CB6 (F$_1$ generation of a BALB/c × C57BL/6 mating). Embryos were then transferred to the oviducts of pseudopregnant females, and the genotype of pups was verified by PCR using transgene-specific primers. Of eight founder lines established with decreased PNA binding to T-cell surfaces, two founder lines were backcrossed to wild-type C57BL/6 mice for at least six generations before further analysis. Eμ-Bcl-2 transgenic [Bcl-2^{Tg}; strain B6.Cg-Tg(BCL2)25Wehi/J] (56), Bim null (Bim$^{\Delta/\Delta}$; strain B6.129-Bcl2l11$^{tm1.1Ast}$/J) (5), and RAG-1 null (Rag$^{\Delta/\Delta}$; strain B6.129S7-Rag1^{tm1Mom}/J) (35) mice were obtained from The Jackson Laboratory (Bar Harbor, ME). GM2/GD2 synthase null (Galgt1$^{\Delta/\Delta}$) mice have been described previously (29) and were provided by the Consortium for Functional Glycomics, grant number GM2116. CD43 null (CD43$^{\Delta/\Delta}$) mice have been described previously (7, 32) and were kindly provided by H. Ziltener (Biomedical Research Centre, University of British Columbia, Vancouver, British Columbia, Canada). Mice lacking core 2 GlcNAcT-1 (C2GNT1$^{\Delta/\Delta}$) and ST3Gal-I (ST3Gal-I $^{\Delta/\Delta}$) have also been previously reported (12, 48). Animals were used between 8 to 12 weeks of age and in compliance with standards and procedures approved by the UCSD Institutional Animal Care and Use Committee.

Cell preparation. Single-cell suspensions were prepared from isolated lymphoid tissues in phosphate-buffered saline (PBS) containing 2% heat-inactivated fetal bovine serum (FBS) after red blood cells lysis with ammonium chloride solution (BD PharM Lyse; BD Biosciences, San Jose, CA). For enrichment of CD8$^+$ T cells, negative depletion using magnetic beads was performed. Briefly, mixed cell suspensions from lymph nodes (pooled from axillary, brachial, cervical, inguinal, and mesenteric lymph nodes) were incubated with biotinylated antibodies to CD4, B220, Mac-1, NK1.1, and Gr-1 (BD Biosciences) and washed with PBS, and labeled cells were depleted with Dynabeads M-280 streptavidin (Invitrogen Co., Carlsbad, CA) according to the manufacturer's recommendations. Resulting cell preparations had a purity of ≥90% CD8$^+$ T cells.

Antibodies, lectins, and flow cytometry. Cells were labeled for flow cytometry using annexin V-allophycocyanin (APC) according to the manufacturer's recommendations (Caltag Laboratories, Burlingame, CA) and in combination with 7-amino-actinomycin D (7-AAD), phycoerythrin (PE)-1B11, PE-CD25 (3C7), PE-CD122 (5H4), PE-CD127 (SB/199), PE- or fluorescein isothiocyanate (FITC)-conjugated anti-CD4 (RM4-5), PE- or APC-conjugated anti-CD8α (53-6.7) (BD Biosciences), or PNA-FITC (Vector Laboratories, Burlingame, CA). Mouse Vβ T-cell receptor (TCR) repertoire analysis was performed with FITC-conjugated antibodies to TCR Vβ 2, 3, 4, 5.1 and 5.2, 6, 7, 8.1 and 8.2, 8.3, 9, 10^b, 11, 12, 13, 14, and 17^a (BD Biosciences). All antibody incubations for flow cytometry were performed on ice for 10 min. In some experiments, cell surface analyses were supplemented with intracellular labeling with PE-conjugated antibodies to either human Bcl-2 (6C8) or Armenian hamster immunoglobulin G isotype control (Ha4/8) using Cytofix/Cytoperm buffer (BD Biosciences) to permeabilize and fix the cells. Data were acquired with a FACSCalibur flow cytometer and analyzed with CellQuest software (BD Biosciences). Polyclonal rabbit anti-Bim antibody (BD Biosciences) was used in Western blotting of total thymocyte lysates.

PCR. ST3Gal-I^{Tg} CD8$^+$ T cells from the lymph node and spleen (purified by negative depletion) were cultured at 37°C with 5% CO$_2$, and aliquots were removed at 0, 24, 48, and 72 h postactivation (for 24 h) with immobilized anti-CD3 (145-2C11, 1 μg/ml; BD Biosciences) in RPMI 1640 media containing 10% heat-inactivated FBS, 1× penicillin–streptomycin–L-glutamine, and 2-mercaptoethanol (Invitrogen). Total RNA was extracted using TRIzol reagent (Invitrogen) and treated with DNase I (DNA-free; Ambion, Austin, TX) to remove any genomic DNA contamination. Reverse transcription was performed using 100 ng total RNA with 40 U Moloney murine leukemia virus (M-MLV) reverse transcriptase containing either oligo(dT)$_{15}$ or random hexamer primers (Promega, Madison, WI) in a final volume of 20 μl. Control reactions lacking reverse transcriptase were performed in parallel. Resulting cDNA from reverse transcription (1 μl) was amplified by PCR using primers specific for the ST3Gal-I transgene or 18s rRNA (QuantumRNA 18s internal standards; Ambion). PCR products were separated on 2% agarose gels, stained with ethidium bromide, and quantified by densitometry.

In vitro T-cell activation. For in vitro apoptosis analysis, cells from lymph nodes or spleen were prepared as described, resuspended in RPMI 1640 media

containing 10% FBS, 1× penicillin–streptomycin–L-glutamine, and 2-mercaptoethanol, and stimulated with immobilized anti-CD3 (145-2C11, 1 μg/ml; BD Biosciences) or ionomycin (0.5 μM)–phorbol myristate acetate (PMA, 10 ng/ml) (Sigma-Aldrich Co., St. Louis, MO) for 24 h in culture at 37°C with 5% CO$_2$. The cells were then removed from activation stimuli, resuspended in fresh media, and further incubated without stimulus for the next 48 h. At this time (72 h postactivation), cells were removed from culture, labeled, and analyzed by flow cytometry. Where indicated, interleukin-2 (50 U/ml; R & D Systems, Minneapolis, MN) was added to the cultures after removal of anti-CD3 at 24 h.

Neuraminidase and lectin application. Lymph node cells (5 × 10^6) from C57BL/6 mice were isolated as described and treated with or without 3 mU protease-free neuraminidase (sialidase) from *Vibrio cholerae* (EC 3.2.1.18; Roche Diagnostics, Indianapolis, IN) in RPMI 1640 media for 25 min at 37°C. After washing with PBS, cells were resuspended at 1 × 10^6 cells/ml in RPMI 1640 media containing PNA, *Erythrina cristagalli* agglutinin (ECA) (Vector Laboratories), or media alone. Where indicated, lectin addition was preceded by a 6-h incubation with immobilized anti-CD3 (145-2C11, 1 μg/ml) or accompanied by D-galactose (25 mM; Sigma-Aldrich). Using live (7-AAD$^−$) CD8$^+$ T cells, annexin V-APC detected phosphatidylserine externalization and caspase activity was assessed by 6-carboxyfluorescein (FAM)–VAD–FMK (Invitrogen) cleavage. DNA fragmentation was measured by terminal deoxynucleotidyltransferase-mediated dUTP-biotin nick end labeling assay (Promega), all according to the manufacturer's recommendations. After 24 h in culture at 37°C with 5% CO$_2$, cells were counted using a hemacytometer and trypan blue exclusion to identify live cells. The proportion of CD8$^+$ T cells in culture was determined by flow cytometry and used in calculating the total CD8$^+$ T-cell count.

LCMV infection. ST3Gal-I^{Tg}, ST3Gal-I$^{\Delta/\Delta}$, and wild-type littermate mice were inoculated with an intraperitoneal injection of 2 × 10^5 PFU of LCMV-Armstrong in 0.2 ml sterile PBS. On days 0, 8, 15, and 30 postinoculation, mice were euthanized, the spleen and lymph nodes were harvested, and cell suspensions were prepared for counting and flow cytometry as described. LCMV-specific T cells were defined by labeling with PE-conjugated D^b gp33-41 major histocompatibility complex (MHC) class I tetramers (Beckman Coulter, Fullerton, CA) and in combination with other markers as described above.

SEB immunization. Mice were injected intravenously on day 0 with 150 μg SEB from *Staphylococcus aureus* (Sigma-Aldrich) in 0.2 ml sterile PBS. On days 0, 2, and 10 postinjection, mice were euthanized, the spleen and lymph nodes were harvested, and cell suspensions were prepared for counting and flow cytometry, as well as used to enrich CD8$^+$ T cells by negative depletion followed by culture in RPMI 1640 as described above. CD8$^+$ T cells expressing the Vβ8 TCR were identified using the PE-conjugated anti-Vβ8 antibody (F23.1; BD Biosciences) and in combination with other antibody markers, as described.

Adoptive transfer of T cells. Thymocytes (5 × 10^6) isolated from Bim$^{\Delta/\Delta}$, ST3Gal-I$^{\Delta/\Delta}$, and Bim$^{\Delta/\Delta}$/ST3Gal-I$^{\Delta/\Delta}$ mice, enriched for double-negative and CD8 single-positive thymocytes (present in identical proportions) as described above, were suspended in 0.2 ml sterile PBS and adoptively transferred into RAG-1-deficient recipient mice (35) by intravenous injection. After 2 weeks, mice were euthanized, and lymphocyte suspensions were prepared from the peripheral blood, lymph nodes, or spleen. CD8$^+$ T cells were identified by antibody labeling, and the percentage of annexin V$^+$ cells was assessed by flow cytometry as described.

RESULTS

Desialylation of core 1 O-glycans sensitizes wild-type CD8$^+$ T cells to apoptotic death by O-glycan cross-linking in vitro. As genetic loss of sialic acid formation on core 1 O-glycans induces CD8$^+$ T-cell apoptosis in vivo, due to ST3Gal-I deficiency, we investigated whether exogenous enzymatic removal of sialic acid from the normal CD8$^+$ T-cell surface increases sensitivity to apoptotic death. Sialidase treatment of wild-type CD8$^+$ T cells removed all cell surface sialic acid linkages without reducing cell viability in vitro and resulted in the exposure of underlying galactose residues among various glycan structures, thereby increasing cell surface expression of ligands for both PNA and ECA lectins (Fig. 1B). The level of PNA ligands induced on wild-type CD8$^+$ T cells treated with sialidase was similar to the level observed among ST3Gal-I-deficient CD8$^+$ T cells, indicating that ST3Gal-I function fully accounts for the
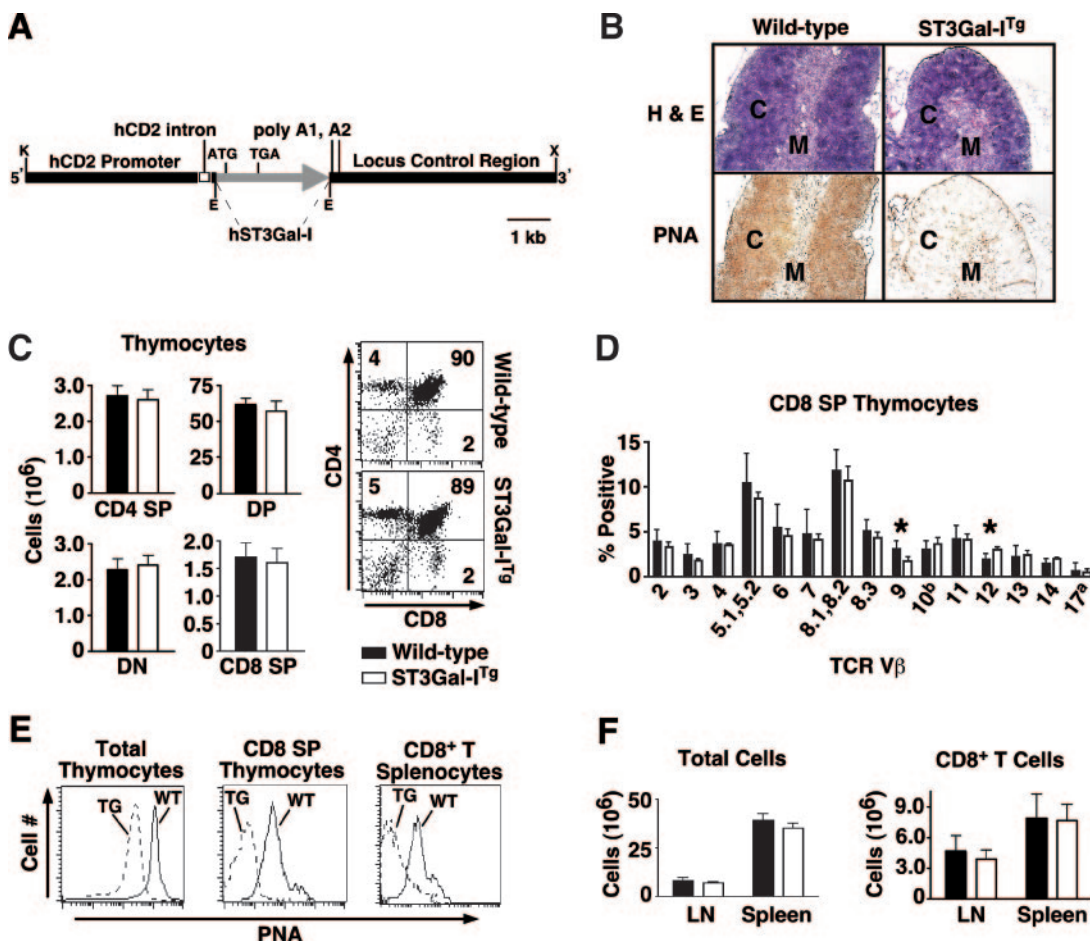
FIG. 2. Constitutive ST3Gal-I transgene expression in T-cell ontogeny and peripheral T-lymphocyte homeostasis. (A) ST3Gal-I transgene construct. The EcoRI fragment of human ST3Gal-I cDNA was inserted into the VA hCD2 minigene cassette, which contains the human CD2 promoter sequence. E, EcoRI; K, KpnI; X, XbaI. (B) Thymic tissue sections from ST3Gal-I^{Tg} animals and wild-type littermates reveal a loss of PNA ligands in both thymic cortex (C) and medulla (M) as a result of constitutive ST3Gal-I expression in T cells. (C) Total thymocyte subset numbers and frequencies among CD4/CD8 double-positive (DP), double-negative (DN), and SP T cells in ST3Gal-I^{Tg} and wild-type littermate mice. (D) TCR Vβ repertoire expression in ST3Gal-I^{Tg} and wild-type littermate CD8 SP thymocyte populations. (E) Analysis by flow cytometry indicates decreased PNA ligands on ST3Gal-I^{Tg} cells compared to littermate control cells among total thymocytes, CD8 SP thymocytes, and CD8$^+$ T cells from spleen. (F) Total cell and CD8$^+$ T-cell numbers in spleen and lymph nodes in ST3Gal-I^{Tg} and wild-type littermate animals. Data are presented as means ± standard errors of the means ($n = 6$). ∗, statistically significant difference from wild-type littermates ($P < 0.05$, paired t test).

sialylation of the Galβ1-3GalNAc core 1 O-glycan. Remarkably, sialidase-treated but not untreated wild-type CD8$^+$ T cells were susceptible to PNA-induced cell death that occurred within 24 h of PNA addition in vitro, matching results obtained using nontreated ST3Gal-I-deficient CD8$^+$ T cells (Fig. 1C). Moreover, cell death was PNA dose dependent and could be inhibited by the addition of free galactose or by TCR activation using anti-CD3 for 6 h prior to sialidase treatment. In contrast, treatment with ECA, which binds to Galβ1-4GlcNAc, failed to induce cell death among sialidase-treated or ST3Gal-I-deficient CD8$^+$ T cells (Fig. 1D), indicating a high degree of specificity for apoptotic signaling involving the O-glycan structure modified by ST3Gal-I. This response is preceded by DNA fragmentation, activation of caspases, and the increased externalization of phosphatidylserine, detected by annexin V binding (Fig. 1E, F, and G) (48). In contrast, CD4$^+$ T cells were not as sensitive to PNA-induced apoptosis, consistent with previous results among ST3Gal-I-deficient mice (data not shown)

(48). These results recapitulate in wild-type CD8$^+$ T cells the acquired sensitivity to apoptosis observed among ST3Gal-I$^{\Delta/\Delta}$ CD8$^+$ T cells and support the view that CD8$^+$ T-cell apoptosis may normally occur among postactivated CD8$^+$ T cells bearing altered O glycosylation.

Constitutive ST3Gal-I transgene expression in T-cell ontogeny and peripheral homeostasis. The model of post-immune CD8$^+$ T-cell apoptosis we previously reported predicts that the apoptosis of CD8$^+$ T cells due to absence of sialic acid on core 1 O-glycan structures would be inhibited by constitutive expression of ST3Gal-I (48). We therefore generated transgenic mice using the human ST3Gal-I cDNA, which is over 90% identical to the mouse sequence, expressed in the T-cell lineage by the human CD2 promoter (Fig. 2A). ST3Gal-I transgenic (ST3Gal-I^{Tg}) mice were viable, fertile, and normal upon examination. Histologic examination of the thymus revealed an overall normal organization and appearance in sections stained with hematoxylin and eosin but a profound reduction in PNA
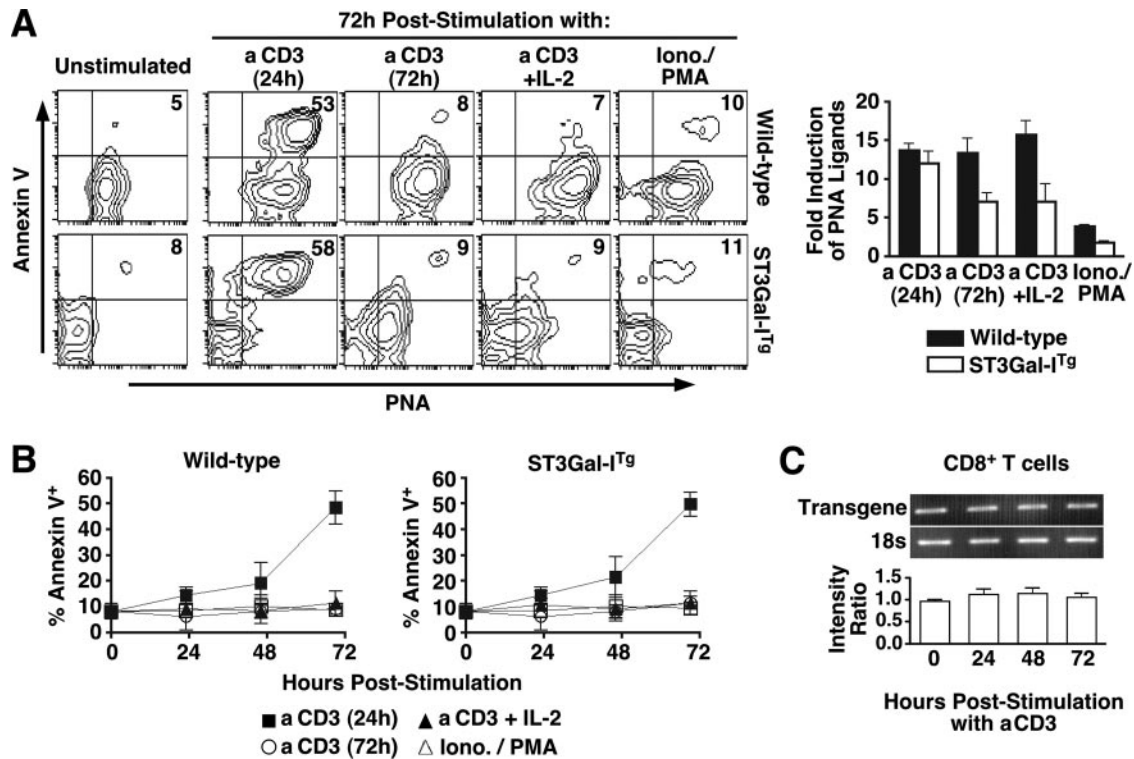
FIG. 3. Annexin V induction in CD8$^+$ T-cell apoptosis is linked to loss of core 1 O-glycan sialylation by a posttranscriptional mechanism. (A) CD8$^+$ T cells from ST3Gal-I^{Tg} and littermate wild-type mice were activated in vitro with the indicated stimuli and analyzed for PNA ligand levels. Flow cytometry plots depict live (7-AAD$^-$) CD8$^+$ T cells; numbers indicate percentages of cells in the upper right quadrant and are representative of results from three separate experiments. PNA ligand levels were assessed by flow cytometry among stimulated cells (at 72 h) and compared to unstimulated CD8$^+$ T cells to calculate relative induction. aCD3, anti-CD3. (B) Percentage of live (7-AAD$^-$) annexin V$^+$ CD8$^+$ T cells at the indicated time points after activation with the indicated stimuli. (C) Reverse transcription-PCR analysis of ST3Gal-I transgene expression (normalized to 18s rRNA expression) was performed on purified CD8$^+$ T cells isolated at 0, 24, 48, and 72 h post-anti-CD3 activation. The intensity ratio represents the ratio of ST3Gal-I transgene to 18S bands as assessed by densitometry.

ligands in both the cortex and medulla, indicative of high-level ST3Gal-I function in thymocytes (Fig. 2B). Elevated ST3Gal-I expression did not significantly affect thymocyte cellularity or ontogeny, judged by CD 4/CD8 subset frequencies (Fig. 2C). The CD8 single-positive (SP) thymocyte population, however, displayed specific alterations in TCR Vβ repertoire expression (Fig. 2D). Notably, frequencies of Vβ9 and Vβ12 were reduced and induced, respectively. These findings are opposite of, and consistent with, those observed in ST3Gal-I-deficient CD8 SP thymocytes and likely reflect alterations proposed in some MHC class I interactions that are modified by CD8 O glycosylation (36). The transgenic increase in core 1 O-glycan sialylation was measured as a three- to fivefold decrease on average in PNA binding to ST3Gal-I^{Tg} thymic and peripheral CD8$^+$ T cells among the spleen, lymph nodes, and blood (Fig. 2E and data not shown). However, this increase in ST3Gal-I function did not significantly alter peripheral lymphoid tissue cellularity or total CD8 T-cell numbers in the lymph nodes or spleen of littermate mice at 8 to 10 weeks of age or those aged for 7 to 12 months (Fig. 2F and data not shown).

Annexin V induction in CD8$^+$ T-cell apoptosis is linked to loss of core 1 O-glycan sialylation by a posttranscriptional mechanism. The appearance of unsialylated core 1 O-glycans on the cell surface of postactivated CD8$^+$ T cells may be inhibited in ST3Gal-I^{Tg} CD8$^+$ T cells bearing constitutive

ST3Gal-I expression. Consistent with this expectation, PNA binding was virtually absent prior to and during early immune activation, reflecting the enhanced level of ST3Gal-I activity. Unexpectedly, however, by 72 h in culture, in vitro immune stimulation with anti-CD3 resulted in a significant increase in unsialylated core 1 O-glycans on ST3Gal-I^{Tg} CD8$^+$ T cells which was comparable to the increase observed on wild-type CD8$^+$ T cells (Fig. 3A). The appearance of the annexin V marker of cell surface phosphatidylserine exposure was always found in association with the induction of PNA ligands that mark the unsialylated core 1 O-glycan. Moreover, the percentage of annexin V$^+$ PNA$^+$ cells could be reduced by either continuous anti-CD3 stimulation or by the addition of exogenous interleukin-2 (IL-2) among wild-type and transgenic CD8$^+$ T cells. Interestingly, stimulation with ionomycin and phorbol ester PMA greatly reduced the appearance of annexin V$^+$ PNA$^+$ CD8$^+$ T cells, implicating the need for TCR stimulation to induce the appearance of unsialylated core 1 O-glycans and further revealing the close link of the annexin V apoptotic marker with the appearance of unsialylated core 1 O-glycans (Fig. 3B). No effect of IL-7 was observed on these responses, and annexin V$^+$ cells were identical to annexin V$^-$ cells in the expression of various receptors for cytokines, including IL-2, IL-15, IL-7, and the common γ chain CD132 (data not shown) (see Fig. S1 in the supplemental material).
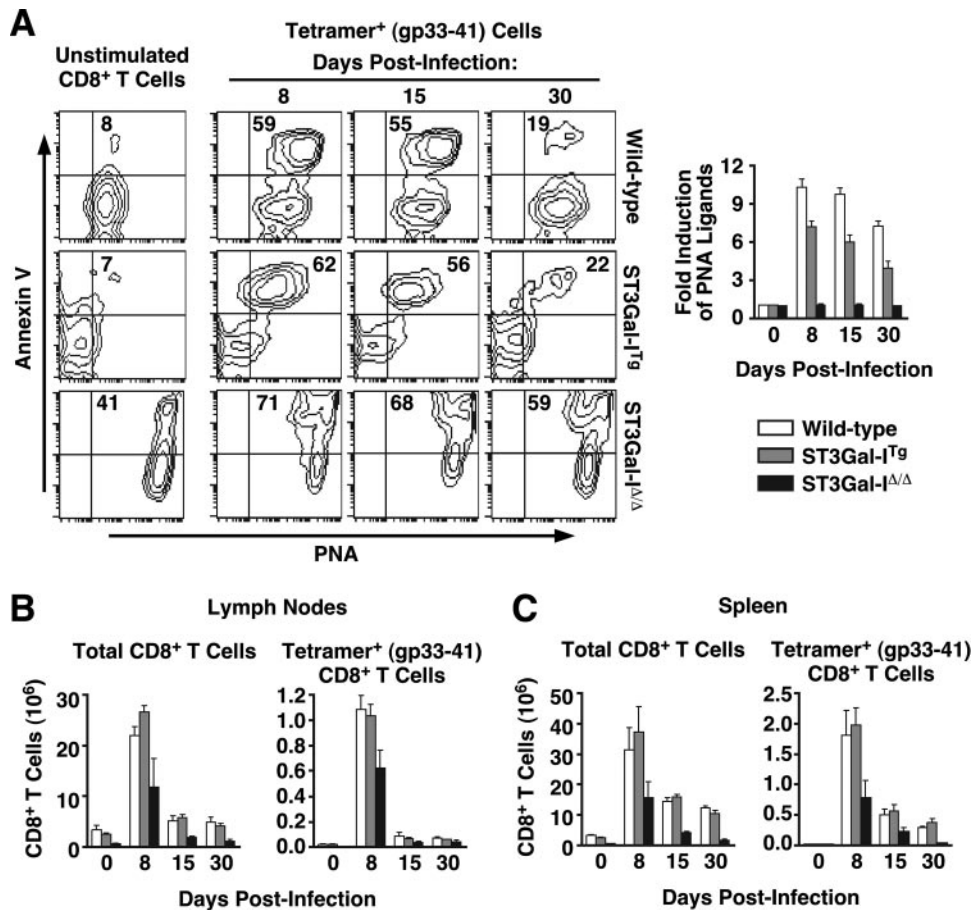
FIG. 4. Relationship of core 1 O-glycans structure to CD8+ T-cell apoptosis following an antiviral immune response in vivo. (A) Live (7-AAD⁻) unstimulated CD8+ T cells (day 0) or gp33-41 tetramer-positive cells (days 8, 15, and 30) labeled with PNA and annexin V. Numbers indicate percentages of cells in the upper right quadrant and are representative of results from three separate experiments. PNA ligand levels were assessed by flow cytometry among gp33-41 tetramer-positive cells (days 8, 15, and 30 postinfection) and compared to unstimulated CD8+ T cells (day 0) to calculate relative induction. Total numbers of CD8+ T cells (left) and CD8+ T cells specific for D^b gp33-41 MHC class I tetramers (right) in lymph nodes (B) and spleens (C) isolated from wild-type, ST3Gal-I^Tg, and ST3Gal-I^{Δ/Δ} mice during LCMV infection are shown. Cells were enumerated by hemacytometer counts in combination with percentages obtained by flow cytometric analysis. Data are presented as means ± standard errors of the means ($n = 3$ to 6).

No significant change was observed in ST3Gal-I transgene mRNA expression throughout the in vitro activation time course (Fig. 3C), suggesting that the appearance of unsialylated core 1 O-glycans on peripheral postactivated CD8+ T cells is due to a posttranscriptional mechanism inactivating ST3Gal-I function or removing the sialic acid linkage produced by ST3Gal-I.

Relationship of core 1 O-glycan structure to CD8+ T-cell apoptosis during an antiviral immune response in vivo. Acute infection of mice with LCMV induces a dramatic clonal expansion of virus-specific CD8+ T cells which peaks 8 days postinfection then undergoes a contraction phase, leaving a stable population of viable memory cells by 30 days postinfection (27, 38). We tested the influence of differential core 1 O-glycan sialylation on this in vivo response by infecting wild-type, ST3Gal-I^Tg, and ST3Gal-I^{Δ/Δ} mice with LCMV and further measuring the level of annexin V binding, which has been used to identify virus-specific CD8+ T cells undergoing apoptosis (60).

We observed a close relationship between unsialylated core

1 O-glycans detected by PNA and annexin V binding on gp33-41 tetramer-positive cells after LCMV infection (Fig. 4A). Moreover, among ST3Gal-I^Tg tetramer-positive cells, only those that expressed unsialylated core 1 O-glycans were positive for annexin V binding, as was observed in vitro upon anti-CD3 activation (Fig. 3A). The induction of unsialylated core 1 O-glycans among gp33-41 tetramer-positive T cells peaked at day 8 in both ST3Gal-I^Tg and wild-type mice with a 6- to 10-fold increase in PNA ligands, respectively, that subsided by day 30, in agreement with previous findings (Fig. 4B) (14, 48). Both wild-type and ST3Gal-I^Tg mice showed similar expansion and contraction responses involving total CD8+ T cells and gp33-41 tetramer-positive CD8+ T cells in the lymph nodes (Fig. 4C) and the spleen (Fig. 4D). Notably, ST3Gal-I^{Δ/Δ} cells, which constitutively displayed unsialylated core 1 O-glycans, also maintained the highest percentage of annexin V⁺ cells throughout the infection time course, which corresponded with low numbers of viable cells in the lymph nodes and spleen at every time point tested. ST3Gal-I^{Δ/Δ} mice also displayed reduced numbers of both total and gp33-41 tetramer-positive
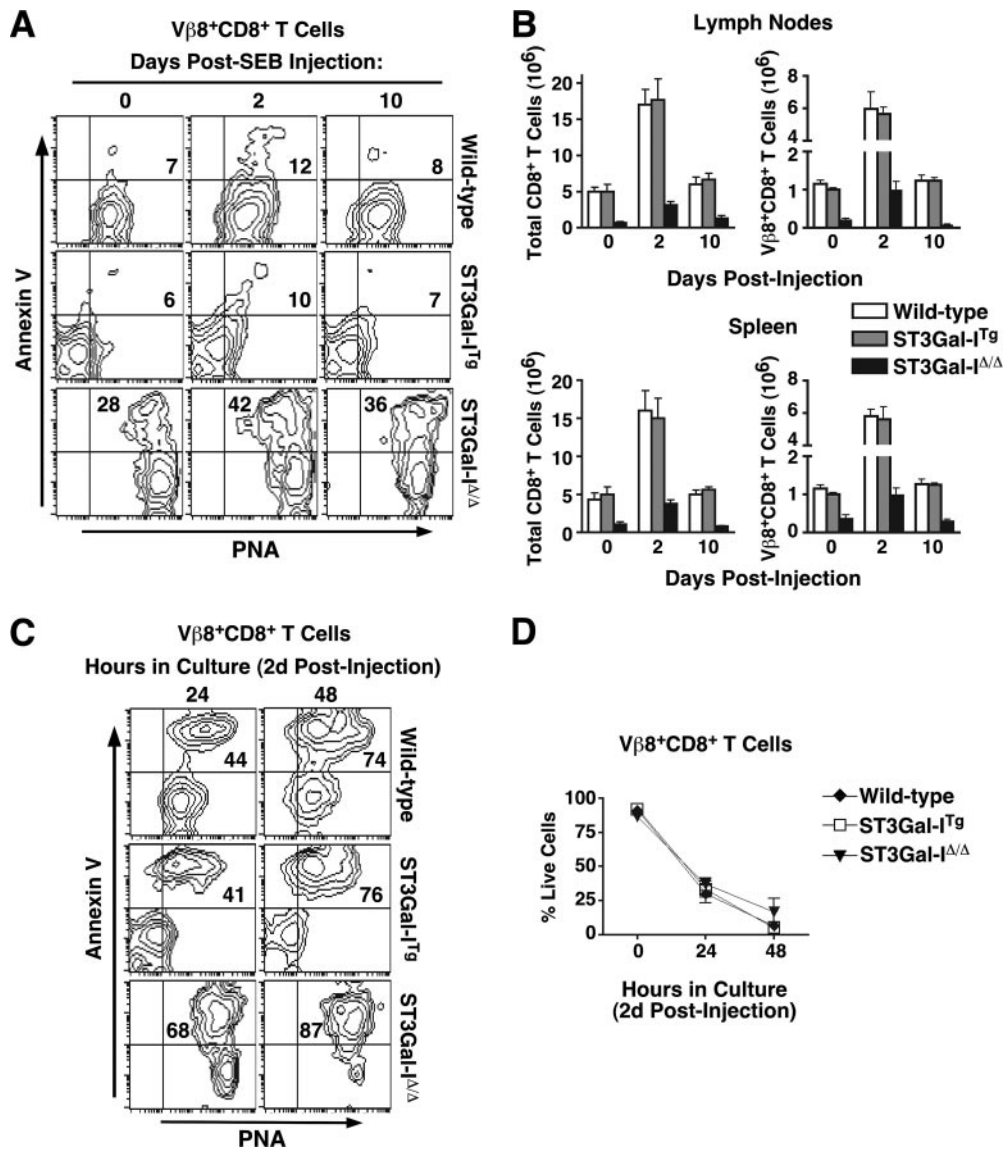
FIG. 5. Relationship of core 1 O-glycan structure to CD8$^+$ T-cell apoptosis following a bacterial antigen-driven immune response in vivo. (A) PNA ligands and annexin V reactivity were assessed by flow cytometry among live (7-AAD$^-$) Vβ8$^+$ CD8$^+$ T cells isolated from wild-type, ST3Gal-I^{Tg}, and ST3Gal-I$^{\Delta/\Delta}$ mice 0, 2, and 10 days post-SEB injection. (B) Total numbers of CD8$^+$ and Vβ8$^+$ CD8$^+$ T cells from the lymph nodes and spleen of wild-type, ST3Gal-I^{Tg}, and ST3Gal-I$^{\Delta/\Delta}$ mice at 0, 2, and 10 days postinjection with SEB. Cells were enumerated by hemacytometer counts in combination with percentages obtained by flow cytometric analysis. (C) PNA ligands and annexin V reactivity were assessed by flow cytometry among live (7-AAD$^-$) Vβ8$^+$ CD8$^+$ T cells removed from wild-type, ST3Gal-I^{Tg}, and ST3Gal-I$^{\Delta/\Delta}$ mice 2 days post-SEB injection and analyzed after 24 or 48 h in culture. Numbers in panels A and C indicate percentages of cells in the upper right quadrant and are representative of results from three separate experiments. (D) Percentage of live (7-AAD$^-$) Vβ8$^+$ CD8$^+$ T cells during the 48 h in culture following isolation at 2 days post-SEB injection. Data in panels B and D are presented as means ± standard errors of the means ($n = 3$).

CD8$^+$ T cells at all time points examined, although distinct expansion and contraction phases involving these cells were observed. These observations are consistent with previous results implicating the normal response of ST3Gal-I-deficient naive CD8$^+$ T cells to TCR stimuli in the presence of attenuated cytotoxic T-cell activity in vivo to MHC-mismatched tumor cell inoculation due to reduced CD8$^+$ T cell numbers (48).

Relationship of core 1 O-glycan structure to CD8$^+$ T-cell apoptosis during a bacterial superantigen-driven immune response in vivo. We investigated the immune response in vivo

upon challenge with SEB superantigen, which recruits CD8$^+$ T cells, including the TCR Vβ8$^+$ population (20). Using wild-type, ST3Gal-I^{Tg}, and ST3Gal-I$^{\Delta/\Delta}$ mice, we found a pattern in the SEB response similar to that observed with LCMV challenge, specifically, all CD8$^+$ T cells that became annexin V$^+$ also expressed unsialylated core 1 O-glycans (Fig. 5A). In addition, the expansion and contraction of Vβ8$^+$ CD8$^+$ T cells displayed similar kinetics among all genotypes (Fig. 5B). When compared to anti-CD3 stimulation or LCMV inoculation, many fewer cells were annexin V$^+$ at the indicated times assayed, although those that were also expressed the highest

levels of unsialylated core 1 O-glycans. Interestingly, the majority of of Vβ8+ CD8+ T cells from both wild-type and ST3Gal-I^{Tg} mice became annexin V+ PNA+ during a subsequent 24- to 48-h culture period ex vivo (Fig. 5C). As with LCMV infection, the corresponding ST3Gal-I$^{Δ/Δ}$ CD8+ T cells constitutively expressed unsialylated core 1 O-glycans, coinciding with a high percentage that were annexin V+ PNA+ throughout the time course. Decreased viable cell numbers upon in vitro culture were comparable among wild-type, ST3Gal-I^{Tg}, and ST3Gal-I$^{Δ/Δ}$ Vβ8+ CD8+ T cells (Fig. 5D). Identical to the in vitro findings, transgenic ST3Gal-I expression in the context of antigen stimulation in vivo maintained sialylated core 1 O-glycans among activated T cells, while apoptotic T cells were both PNA+ and annexin V+.

Assigning O-glycan structure, secretory pathway positioning, and protein- or lipid-linkage participation in CD8+ T-cell apoptosis. Concurrent with the induction of unsialylated core 1 O-glycans following immune activation, CD8+ T cells induce core 2 O-glycans on the cell surface, which is enabled in part by elevated core 2 GlcNAcT-1 expression (Fig. 1A) (47, 48). Thus, the specific O-glycan structure that induces apoptosis and which may be a ligand for an endogenous lectin, might include both core 1 and core 2 branch modifications. To further resolve the glycan structure required for inducing CD8+ T-cell apoptosis, we analyzed CD8+ T-cell numbers and apoptotic markers among core 2 GlcNAcT-1-deficient mice and those further lacking ST3Gal-I. Similar studies with multiple gene deficiency states were performed in mice lacking the CD43 glycoprotein or Galgt1-dependent glycolipids. CD43 is a major carrier of core 1 O-glycans along with induced levels of core 2 O-glycan branching (47). In addition, Galgt1-dependent glycolipid structures have been found to bind to the PNA lectin (1), and therefore, mice lacking this glycosyltransferase were also examined.

The absence of core 2 GlcNAcT-1 failed to restore normal CD8+ T cell levels in mice also lacking ST3Gal-I. Identical results were observed among mice lacking either CD43 or Galgt1 in the context of ST3Gal-I deficiency (Fig. 6A). Restoration of normal CD8+ T-cell homeostasis was achieved, however, in ST3Gal-I-deficient mice bearing the human ST3Gal-I transgene. Levels of core 2 O glycosylation, unsialylated core 1 O-glycans, and annexin V binding were also measured in these resting and activated CD8+ T cells. Remarkably, transgenic ST3Gal-I expression blocked the induction of core 2 O-glycans that are produced in the medial Golgi apparatus following immune activation (Fig. 6B) (48). As increased PNA ligand formation and annexin V binding continues among CD8+ T cells in ST3Gal-I^{Tg} mice, we can conclude that core 2 O-glycan branching is not a determinant in the glycan structure contributing to peripheral homeostasis in postactivated CD8+ T cells. Identical results were obtained among ST3Gal-I^{Tg} CD8+ T cells during the in vivo immune response to LCMV (data not shown). CD43 deficiency also failed to diminish the induction of unsialylated core 1 O-glycans and annexin V binding, while the level of core 2 O-glycans apportioned to this glycoprotein appeared to reflect more than 60% of the level typically induced following activation. In addition, there was no contribution to CD8+ T-cell homeostasis evident among mice lacking glycolipids produced by Galgt1 or in collaboration with ST3Gal-I.

Loss of ST3Gal-I overcomes Bcl-2 expression to induce CD8+ T-cell apoptosis in vivo, but not in vitro, coincident with expression of unsialylated core 1 O-glycans. Previous studies have demonstrated that transgenic expression of Bcl-2 in T cells protects them from apoptosis in vitro and after immune stimulation in vivo (21, 56). To further identify the molecular circuitry involved in CD8+ T-cell apoptosis, we generated ST3Gal-I-deficient mice that also expressed a T-cell-specific human Bcl-2 transgene (56) and examined peripheral CD8+ T-cell numbers. We confirmed that the Bcl-2 transgene was expressed similarly in both Bcl-2^{Tg} and Bcl-2^{Tg}/ST3Gal-I$^{Δ/Δ}$ CD8+ T cells (see Fig. S2A in the supplemental material). Bcl-2 transgene expression did not reduce the high level of PNA ligands or decrease the percentage of annexin V+ CD8+ T cells in Bcl-2^{Tg}/ST3Gal-I$^{Δ/Δ}$ mice, compared with ST3Gal-I deficiency alone (Fig. 7A). A significant decrease in peripheral CD8+ T cells was observed in ST3Gal-I-deficient mice regardless of the presence of the Bcl-2 transgene, while no differences were observed in the CD4+ T-cell population (Fig. 7B and C).

We further determined whether the presence of the Bcl-2 transgene would inhibit the post-immune contraction of CD8+ T cells by apoptosis in response to SEB. In agreement with reported findings, the Bcl-2 transgene by itself reduced contraction of Vβ8+ CD8+ T cells in the post-immune contraction phase of the response among the lymph nodes and spleen, compared with wild-type littermates. Remarkably, however, Vβ8+ CD8+ T-cell contraction was reestablished in Bcl-2^{Tg} mice that lacked ST3Gal-I, similar to findings in ST3Gal-I-deficient controls (Fig. 7D). The degree of cell contraction was directly proportional to the frequency of cells bearing unsialylated core 1 O-glycans concurrent with the induction of annexin V binding (Fig. 7E). Nevertheless, when activated Vβ8+ CD8+ T cells were removed at 2 days post-SEB injection and placed in culture for 2 days, the viable cell number was highest among both Bcl-2^{Tg} and Bcl-2^{Tg}/ST3Gal-I$^{Δ/Δ}$ Vβ8+ CD8+ T cells, remaining indirectly proportional to apoptotic marker expression among Vβ8+ CD8+ T cells from wild-type and ST3Gal-I-deficient mice (Fig. 7F and data not shown).

ST3Gal-I deficiency attenuates the accumulation of CD8+ T cells in the absence of Bim. Unlike Bcl-2 transgenic mice, Bim-deficient mice accumulate lymphocytes even among experimentally and immunologically naive animals (5). The presence or absence of Bim was verified among all genotypes (see Fig. S2B in the supplemental material). We further examined mice deficient in both ST3Gal-I and Bim and compared results with littermates that were either wild type or deficient in either ST3Gal-I or Bim alone. Peripheral CD8+ T cells from Bim-deficient mice expressed low levels of annexin V binding, similar to Bcl-2 transgenic cells. In contrast to results obtained with the Bcl-2 transgene, Bim deficiency significantly reduced the frequency of annexin V+ CD8+ T cells in the absence of ST3Gal-I, compared with ST3Gal-I deficiency alone (Fig. 8A). This coincided with restoration of splenic CD8+ T cell numbers to wild-type levels, while lymph node CD8+ T-cell cellularity was increased by more than twofold to about 50% of normal (Fig. 8B). These findings were specific to the CD8+ T-cell population, as CD4+ T cells continued to accumulate excessively in the absence of Bim, regardless of ST3Gal-I function (Fig. 8C).
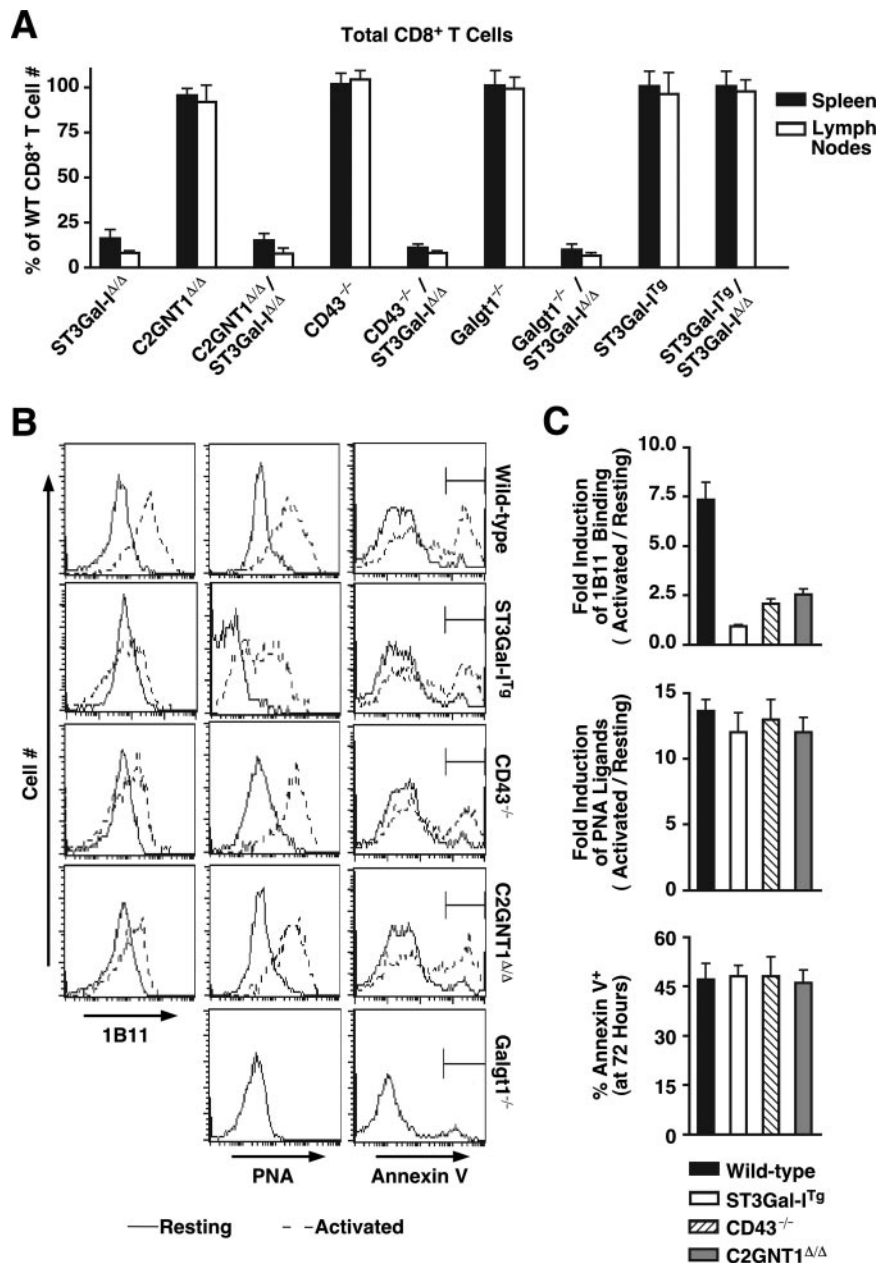
FIG. 6. O-glycan structure, secretory pathway positioning, and protein- or lipid-linkage participation in CD8$^+$ T-cell apoptosis. (A) Peripheral deficiency of CD8$^+$ T cells observed in ST3Gal-I deficiency is rescued by transgenic expression of ST3Gal-I but is not altered in the absence of CD43, core 2 GlcNAcT-1 (C2GNT1), or Galgt1. Total CD8$^+$ T-cell numbers in the lymph nodes and spleen are represented as a percentage of the number obtained from wild-type littermate mice. (B) Activation-induced formation of 1B11-reactive core 2 O-glycans is inhibited in ST3Gal-I^{Tg} CD8$^+$, CD43$^{-/-}$, and C2GNT1$^{\Delta/\Delta}$ CD8$^+$ T cells; however, PNA ligands continue to appear coincident with the normal induction of apoptotic annexin V-positive cells. Histograms in panel B show live (7-AAD$^-$) CD8$^+$ T cells in a resting state (solid lines) and 72 h post-anti-CD3 activation (dotted line; as described for Fig. 3). (C) Relative induction of 1B11 antibody binding and PNA ligands between resting and activated cells and percentages of annexin V$^+$ cells are presented as means ± standard errors of the means ($n = 3$). Data in panel A are presented as means ± standard errors of the means ($n = 6$).

Bim deficiency was previously shown to protect CD8$^+$ T cells from death following in vivo SEB challenge (21). Therefore, we next examined whether ST3Gal-I deficiency altered this phenotype among mice also lacking Bim. As expected, Bim deficiency prevented the apoptotic post-immune contraction of Vβ8$^+$ CD8$^+$ T cells compared with wild-type littermates in the spleen and the lymph nodes. Remarkably, while the contrac-

tion response was restored in the lymph nodes by ST3Gal-I deficiency, Vβ8$^+$ CD8$^+$ T-cell contraction in the spleen remained inhibited (Fig. 8D). These differing effects of CD8$^+$ T-cell contraction apportioned to specific tissue types nevertheless correlated with the frequencies of CD8$^+$ T cells that expressed high levels of both unsialylated core 1 O-glycans and the annexin V apoptotic marker (Fig. 8E). Interestingly, in
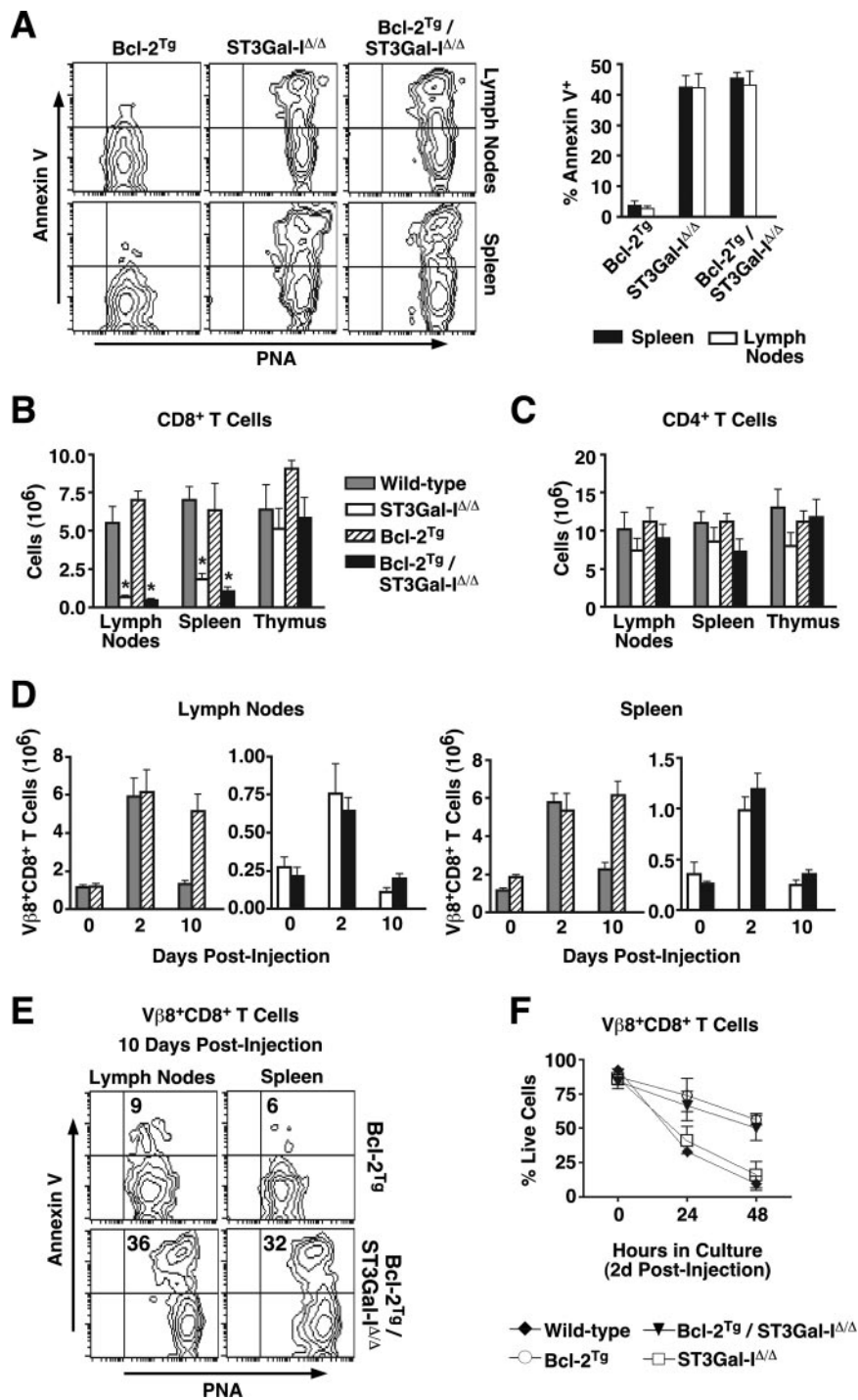
FIG. 7. Loss of ST3Gal-I overcomes Bcl-2 expression to induce CD8^{+} T-cell apoptosis in vivo, but not in vitro, coincident with the expression of unsialylated core 1 O-glycans. (A) Flow cytometric analysis of live (7-AAD^{−}) CD8^{+} cells from the lymph nodes and spleens of wild-type, Bcl-2[Tg], ST3Gal-I[Δ/Δ], and Bcl-2[Tg]/ST3Gal-I[Δ/Δ] mice. Percentages of annexin V^{+} cells are shown in the graph at the right depicting means ± standard errors of the means ($n = 4$). Total numbers of CD8 (B) and CD4 (C) SP cells from the lymphoid tissues of wild-type, Bcl-2[Tg], ST3Gal-I[Δ/Δ], and Bcl-2[Tg]/ST3Gal-I[Δ/Δ] mice. (D) Total numbers of Vβ8^{+} CD8^{+} T cells from lymph nodes and spleens of indicated mice at 0, 2, and 10 days postinjection with SEB. (E) PNA ligands and annexin V reactivity were assessed by flow cytometry among live (7-AAD^{−}) Vβ8^{+} CD8^{+} T cells removed from Bcl-2[Tg] and Bcl-2[Tg]/ST3Gal-I[Δ/Δ] mice 10 days post-SEB injection. (F) Percentages of live (7-AAD^{−}) Vβ8^{+} CD8^{+} T cells during the 48 h in culture following isolation at 2 days post-SEB injection. In all cases, cells were enumerated by hemacytometer counts in combination with percentages obtained by flow cytometric analysis. Data are presented as means ± standard errors of the means ($n = 6$ [A to C] and $n = 3$ [D, F]). *, statistically significant difference from wild-type littermates ($P < 0.05$, unpaired t test).
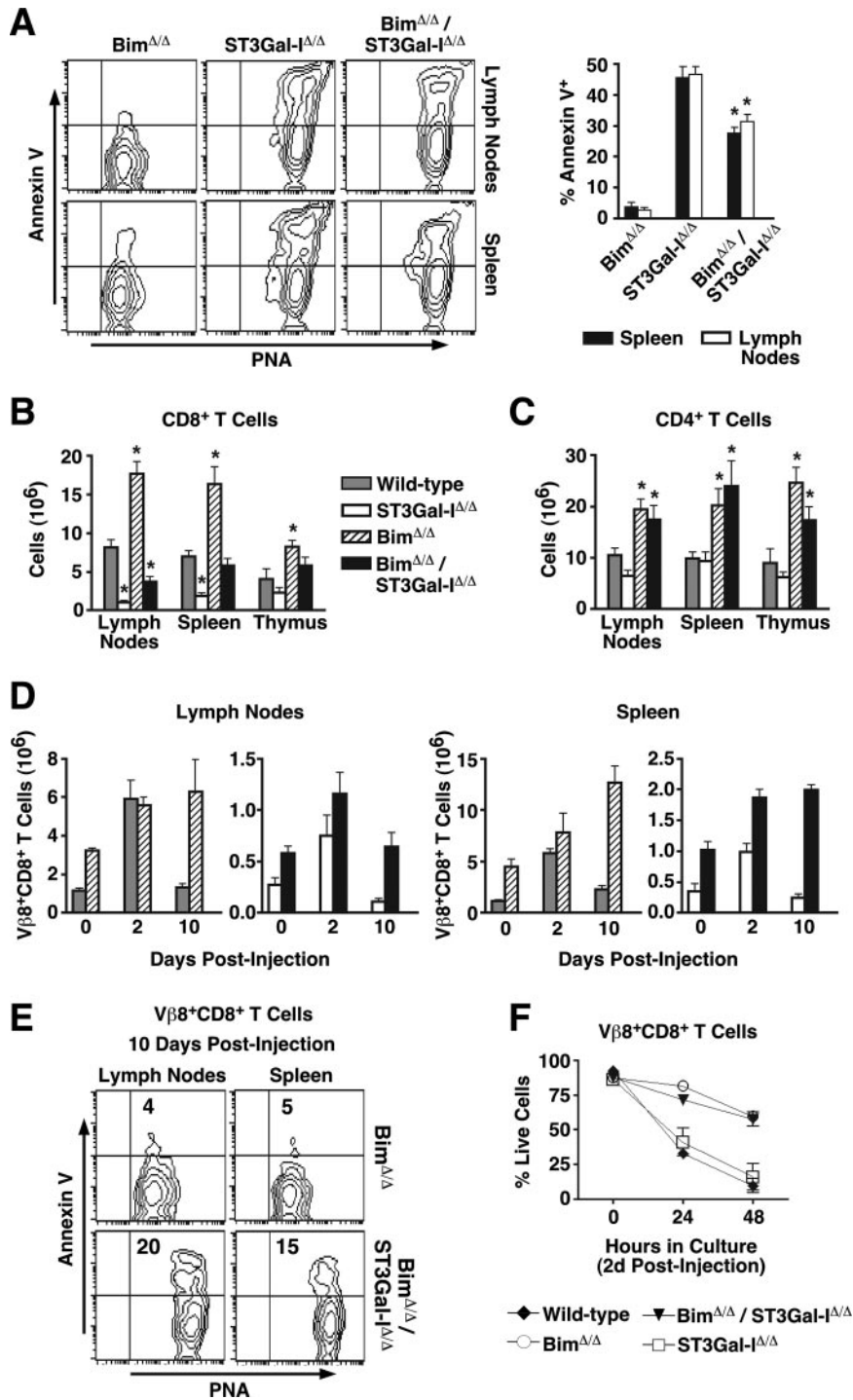
FIG. 8. ST3Gal-I deficiency attenuates the accumulation of CD8$^+$ T cells in the absence of Bim. (A) Flow cytometric analysis of live (7-AAD$^-$) CD8$^+$ cells from the lymph nodes and spleens of wild-type, Bim$^{\Delta/\Delta}$, ST3Gal-I$^{\Delta/\Delta}$, and Bim$^{\Delta/\Delta}$/ST3Gal-I$^{\Delta/\Delta}$ mice. The percentages of annexin V$^+$ cells are shown in the graph at right depicting means ± standard errors of the means ($n = 4$). Total numbers of CD8 (B) and CD4 (C) SP cells from lymphoid tissues of wild-type, Bim$^{\Delta/\Delta}$, ST3Gal-I$^{\Delta/\Delta}$, and Bim$^{\Delta/\Delta}$/ST3Gal-I$^{\Delta/\Delta}$ mice. (D) Total numbers of Vβ8$^+$ CD8$^+$ T cells from the lymph nodes and spleens of indicated mice at 0, 2, and 10 days postinjection with SEB. (E) PNA ligands and annexin V reactivity were assessed by flow cytometry among live (7-AAD$^-$) Vβ8$^+$ CD8$^+$ T cells removed from Bim$^{\Delta/\Delta}$ and Bim$^{\Delta/\Delta}$/ST3Gal-I$^{\Delta/\Delta}$ mice 10 days post-SEB injection. (F) Percentages of live (7-AAD$^-$) Vβ8$^+$ CD8$^+$ T cells during the 48 h in culture following isolation at 2 days post-SEB injection. In all cases, cells were enumerated by hemacytometer counts in combination with percentages obtained by flow cytometric analysis. Data are presented as means ± standard errors of the means ($n = 6$ [A to C] and $n = 3$ [D, F]). ∗, statistically significant difference from ST3Gal-I$^{\Delta/\Delta}$ (in panel A) or wild-type littermates (in panels B and C) ($P < 0.05$, unpaired t test).
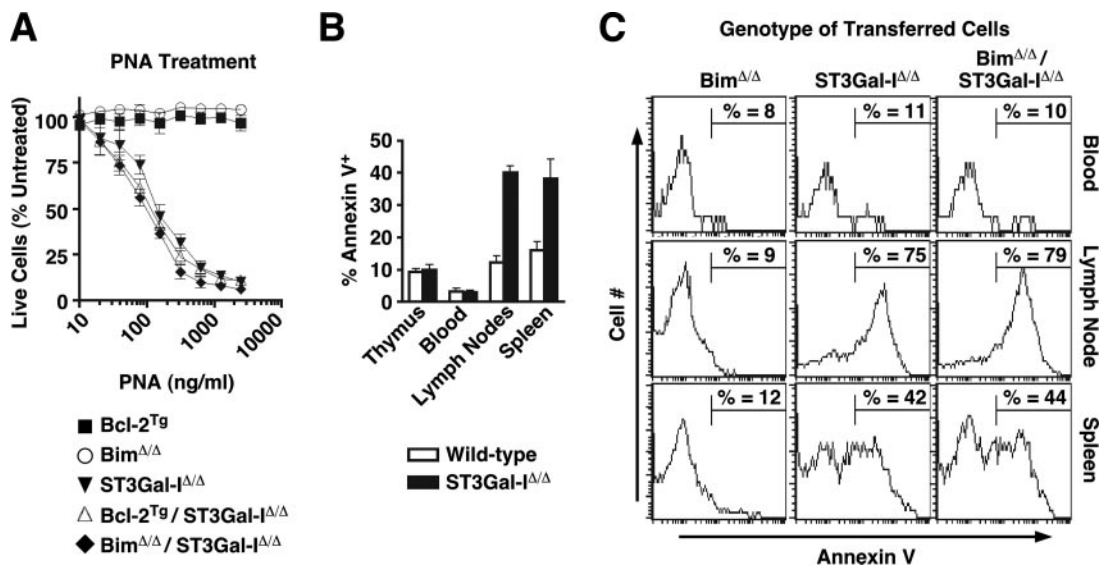
FIG. 9. Dose-response induction of apoptosis and apoptotic CD8+ T-cell compartmentalization. (A) Cross-linking of the unsialylated core 1 O-glycan Galβ1-3GalNAcα-Ser/Thr induces death in ST3Gal-I$^{\Delta/\Delta}$, Bcl-2^{Tg}/ST3Gal-I$^{\Delta/\Delta}$, or Bim$^{\Delta/\Delta}$/ST3Gal-I$^{\Delta/\Delta}$, but not in Bcl-2^{Tg} or Bim$^{\Delta/\Delta}$ CD8+ T cells (incubated with PNA, as in Fig. 1C). Cell counts are presented as percentages (means ± standard errors of the means; $n = 3$) of live CD8+ T cells compared to control cultures not treated with lectin. (B) Percentages of CD8 SP T cells positive for annexin V upon isolation from the thymus, peripheral blood, lymph nodes, or spleen of ST3Gal-I$^{\Delta/\Delta}$ or wild-type littermate mice (means ± standard errors of the means; $n = 3$). (C) CD8 SP thymocytes isolated from the indicated mice were adoptively transferred into $Rag1^{\Delta/\Delta}$ recipients and recovered after 2 weeks from the peripheral blood, lymph nodes, or spleen, and the percentages of annexin V+ cells (gating shown) were assessed by flow cytometry.

vitro culture of Vβ8+ CD8+ T cells revealed that Bim deficiency reduced cell death in vitro independent of ST3Gal-I, similar to findings with Bcl-2 transgenic T cells, and with cell survival also indirectly proportional to the frequency of cells expressing both unsialylated core 1 O-glycans and annexin V (Fig. 8F and data not shown).

Induction of apoptotic CD8+ T cells in dose-response O-glycan cross-linking, among cell compartments, and in the leukopenic state. The phenotypic modulation of CD8+ T-cell apoptosis in ST3Gal-I deficiency by Bcl-2 and Bim may be explained by the expression of an endogenous stimulus more abundant in the lymph nodes than in the spleen and absent from in vitro cell cultures. Such a stimulus may be a lectin, similar in specificity to PNA, that cross-links one or more key O-glycoproteins bearing unsialylated core 1 O-glycans and thereby induces apoptosis. Alternatively, Bim and Bcl-2 may reside in partial epistatic relationships with ST3Gal-I within apoptotic signaling pathways that contribute to the post-immune CD8+ T-cell contraction phase. To further discern among such possibilities, we explored the dose-response relationship of CD8+ T cells from Bcl-2 transgenic and Bim-deficient mice in the presence or absence of ST3Gal-I. No reduction was observed in the sensitivity to PNA-induced annexin V induction or cell death in vitro, implying that neither increasing Bcl-2 expression nor Bim deficiency alters the efficacy of apoptotic signaling invoked by cross-linking glycoproteins bearing unsialylated core 1 O-glycans (Fig. 9A). In addition, there remained significant differences in the frequency of apoptotic cells among different peripheral compartments of wild-type and ST3Gal-I-deficient mice, similar to those seen in the absence of Bim, with the highest frequencies of annexin V+ cells

in the spleen and lymph nodes compared to thymus and blood (Fig. 9B).

These findings implied that an endogenous apoptotic stimulus may be restrictively expressed and in limited supply. We therefore transplanted equal numbers of viable T cells of different genotypes into RAG-1-deficient mice, which lack lymphocytes, and measured the frequency of annexin V+ CD8+ T cells during the early phases of lymphocyte expansion, when peripheral lymphoid tissues were colonized by fewer T cells than in normal naive and immunized wild-type mice. Remarkably, the reduced frequency of annexin V+ CD8+ T cells detected in the absence of both Bim and ST3Gal-I failed to occur, and equally high levels of annexin V+ CD8+ T-cell numbers were observed compared to ST3Gal-I deficiency alone (Fig. 9C). Moreover, and similar to results for Bim-deficient mice, the frequency of CD8+ T cells expressing the annexin V apoptotic marker was highest in the lymph nodes, followed by the spleen, whereas a very low percentage of annexin V+ CD8+ T cells was observed in peripheral blood. These results support a model of CD8+ T-cell apoptosis wherein loss of the sialic acid produced by ST3Gal-I on core 1 O-glycans exposes a ligand for a limited number of endogenous lectins that cross-link one or more O glycoproteins in inducing annexin V expression and caspase activation (Fig. 10).

DISCUSSION

Modulation of protein O glycosylation on the postactivated T-cell surface is closely linked to peripheral CD8+ T-cell apoptosis and appears to play a significant role in the contraction phase of the immune response. We have extended our initial
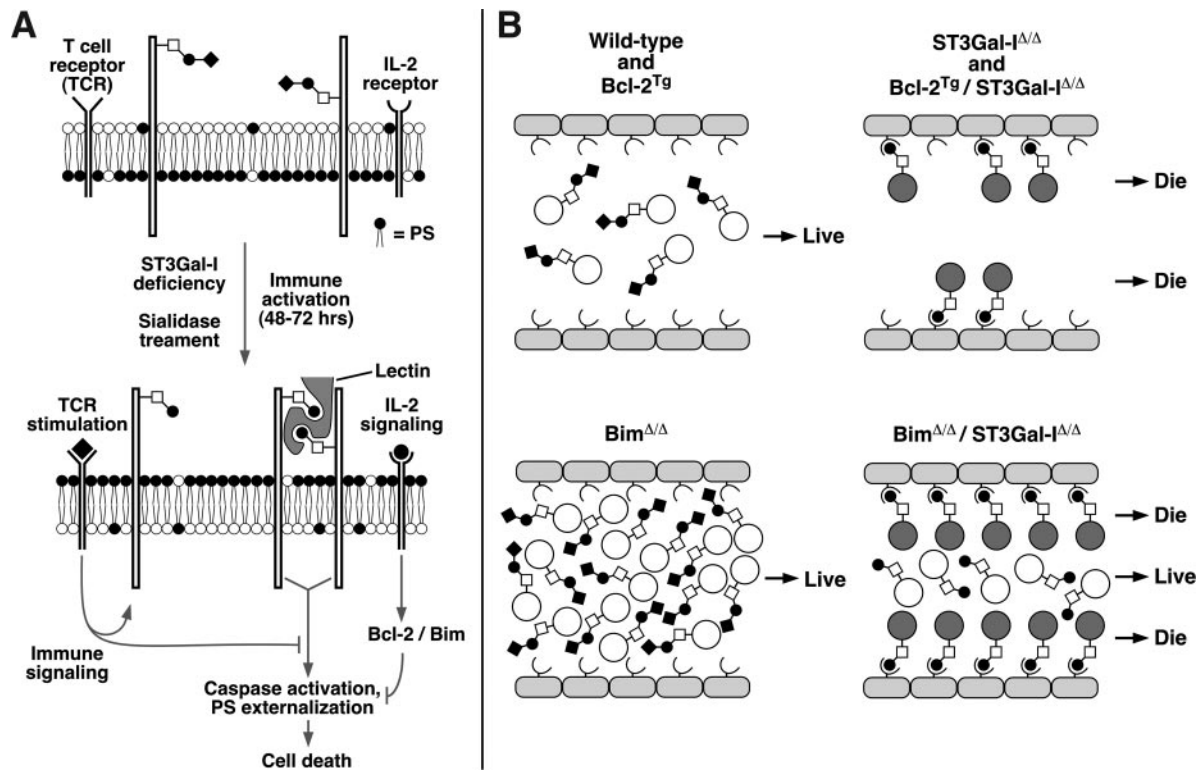
FIG. 10. Model of ST3Gal-I function in CD8$^+$ T-cell apoptosis. (A) Absence of core 1 O-glycan sialylation by reduced ST3Gal-I function induces a glycan ligand for an endogenous multivalent lectin that cross-links specific O-glycoproteins bearing unsialylated core 1 O-glycans to induce apoptosis. TCR stimulation and IL-2 signaling block this apoptotic signal, which may partially overlap with Bcl-2 function but appears predominantly independent of Bcl-2 and Bim. PS, phosphatidylserine. (B) This may reflect the presence of limiting levels of an endogenous multivalent lectin expressed among peripheral lymphoid tissues. Levels of peripheral nonactivated CD8$^+$ T cells in the various experimental genotypes reflect the presence or absence of O-glycan lectin ligands modulated by ST3Gal-I. A reduction of viable CD8$^+$ T-cell numbers to those similar in wild-type mice is thereby achieved in the hyperaccumulation phenotype of Bim deficiency.

report that identified the ST3Gal-I sialyltransferase as regulating this O-glycan alteration and have found evidence that apoptosis among wild-type CD8$^+$ T cells is also linked with this same O-glycan change, following both in vitro and in vivo immune stimulation regimens. Unexpectedly, this change in protein O glycosylation is controlled by a novel posttranscriptional mechanism that regulates ST3Gal-I function subsequent to core 2 O-glycan formation in the medial Golgi apparatus. This has allowed us to identify the minimal O-glycan structure that is sufficient to induce apoptosis as an unsialylated core 1 O-glycan. The relationship of this O-glycan structure to mechanisms inducing apoptosis suggests a ligand for an endogenous saturable lectin is expressed differentially among lymphoid compartments in vivo. The molecular mechanism of action in vivo overrides Bcl-2 transgene expression and Bim deficiency to a significant extent, implicating an extrinsic apoptotic pathway modulated by ST3Gal-I function.

Relationship of CD8$^+$ T-cell apoptosis to altered protein O glycosylation. Following immune activation in vitro or in vivo, both CD4$^+$ and CD8$^+$ T cells produce a measurable change in protein O glycosylation detected by a 10- to 20-fold increase in PNA lectin binding to the intact cell surface. Nevertheless, induction of unsialylated core 1 O-glycans induces apoptosis only among the CD8$^+$ T-cell population in mice lacking ST3Gal-I (48). We have now found that producing this O-

glycan change by cell surface desialylation of wild-type CD8$^+$ T cells sensitizes them to PNA-induced apoptosis, which is preceded by the induction of DNA fragmentation, caspase activation, and phosphatidylserine externalization. The specificity of this response to unsialylated core 1 O-glycans was evident as increased ECA lectin binding to other galactose-bearing glycan branch termini also occurred upon sialidase treatment but failed to alter cell viability, eliminating the possibility of a nonspecific effect of global desialylation.

The acquisition of the annexin V$^+$ cell surface phenotype with induced levels of PNA$^+$ unsialylated core 1 O-glycans tracked directly with frequencies of apoptotic death and reduced peripheral CD8$^+$ T-cell numbers in all genotypes of CD8$^+$ T cells studied. This O-glycan determinant of apoptotic fate is present 48 to 72 h following TCR stimulation but does not likely participate in immune activation, as constitutive transgenic expression of ST3Gal-I results in PNA$^-$ T cells that respond normally to immune stimuli. This O-glycan change, however, invariably precedes apoptosis in the absence of recent TCR stimulation, and when immune signals appear to be waning, as in the context of limiting IL-2 levels. Interestingly, this change in protein O glycosylation may require direct TCR stimulation, as ionomycin and PMA treatment, which activates T cells but bypasses direct TCR stimulation, fails to induce

unsialylated core 1 O-glycans coincident with reduced apoptotic death.

The close relationship of annexin V binding on CD8$^+$ T cells with the increased presence of unsialylated core 1 O-glycans was further evident upon in vivo immune activation by viral challenge (LCMV) and bacterial superantigen (SEB) immunization. In all studies, clonal expansion was followed by a measurable contraction phase, the latter being proportional to the frequency of PNA$^+$ annexin V$^+$ CD8$^+$ T cells among the relevant responding populations. TCR stimulation by viral or bacterial antigens invariably elevated unsialylated core 1 O-glycan levels prior to increased annexin V binding, which together marked apoptotic cell frequencies that correlated directly with total viable peripheral cell numbers. Remarkably, transgenic ST3Gal-I expression again abolished the appearance of unsialylated core 1 O-glycans among activated CD8$^+$ T cells but not among the apoptotic annexin V$^+$ population that is increased in frequency during the contraction phase. As previously indicated in multiple genotypes and contexts, viable CD8$^+$ T cells remaining following the contraction phase may be memory CD8$^+$ T cells, which are more similar to resting CD8$^+$ T cells in having increased levels of sialic acid on cell surface core 1 O-glycans (14, 48).

Structure and regulation of protein O glycosylation in CD8$^+$ T-cell apoptosis. The appearance of unsialylated core 1 O-glycans following TCR stimulation is normally accompanied by an induction of core 2 O-glycan branching (47). We have now shown that core 2 O-glycan branching is not involved in CD8$^+$ T-cell apoptosis as induced by the absence of ST3Gal-I. Core 2 GlcNAcT-1 deficiency did not affect CD8$^+$ T-cell homeostasis or rescue peripheral CD8$^+$ T-cell numbers in mice also deficient in ST3Gal-I. The frequency of CD8$^+$ T cells that were PNA$^+$ annexin V$^+$ remained elevated, similar to ST3Gal-I deficiency alone. The normal induction of core 2 O-glycan branching upon T-cell activation may modulate the production of selectin ligands that regulate lymphocyte trafficking (55). This finding implicates the unsialylated core 1 O-glycan Galβ1-3GalNAc-Ser/Thr as a glycan structure that controls apoptotic signaling in CD8$^+$ T cells.

Efforts to block the loss of sialic acid on core 1 O-glycans following CD8$^+$ T-cell activation involved the successful production of ST3Gal-I transgenic mice bearing constitutive ST3Gal-I function throughout T-cell ontogeny and immune stimulation. Human ST3Gal-I enzyme function in the mouse thymus was evident, along with the ability of the human transgene to rescue CD8$^+$ T-cell numbers in the absence of endogenous mouse ST3Gal-I. The loss of PNA binding in cortical thymoyctes correlated with changes in the same TCR Vβ chains affected in ST3Gal-I deficiency and, in an opposing manner, consistent with a role for ST3Gal-I activity in altering CD8-MHC interactions (36, 37). These relatively minor changes in the TCR Vβ repertoire, however, did not alter mature T-cell activation responses (data not shown). Unexpectedly, elevated and constitutive ST3Gal-I expression blocked the appearance of 1B11 binding determinants upon CD8$^+$ T-cell activation that require core 2 GlcNAcT-1, supporting the view that ST3Gal-I competes with core 2 GlcNAcT-1 for glycoprotein substrates in vivo (48, 51).

Remarkably, increased ST3Gal-I expression fails to inhibit the appearance of unsialylated core 1 O-glycans on postacti-

vated CD8$^+$ T cells. This finding implies that loss of ST3Gal-I function following CD8$^+$ T-cell stimulation reflects a posttranscriptional regulatory mechanism. The ability of the transgene to compete with core 2 GlcNAcT activity in the medial Golgi apparatus and sialylate all core 1 O-glycans in resting CD8$^+$ T cells reveals that unsialylated core 1 O-glycans likely result from an event that occurs in the late (*trans*) Golgi network or in post-Golgi processing. This is consistent with the absence of significant difference in endogenous ST3Gal-I mRNA levels among resting and activated wild-type CD8$^+$ T cells (1). Elevated levels of unsialylated core 1 O-glycans may reflect increased sialidase activity upon T-cell activation (14, 26, 59); however, other studies have found that absence of specific sialidase function, or broad inhibition of sialidase activity, had no effect on the appearance of unsialylated core 1 O-glycans and instead implicated a de novo process by which newly synthesized glycoproteins lack sialic acids on core 1 O-glycans (1). Efforts to produce antibodies to investigate glycosyltransferase regulation have been mostly unsuccessful, but such reagents will be needed to more fully define the mechanisms controlling ST3Gal-I function.

Mechanism of apoptotic regulation by ST3Gal-I. It is clear that not all glycoproteins normally bearing unsialylated core 1 O-glycans participate in CD8$^+$ T-cell apoptosis. We have found that the CD43 glycoprotein, which carries unsialylated core 1 O-glycans in addition to the majority of core 2 O-glycans induced following CD8$^+$ T-cell activation, and has been implicated in apoptosis (6, 42, 48), does not participate in apoptosis among ST3Gal-I-deficient CD8$^+$ T cells. In addition, the susceptibility of CD8$^+$ T cells to PNA-induced apoptosis was not altered by the addition of IL-7 and did not coincide with altered expression levels of various cytokine receptors (data not shown). Among glycoprotein candidates other than CD43, both CD8 and CD45 are also modified with unsialylated core 1 O-glycans (1, 8, 36, 37, 48, 61). Recently, cross-linking of CD8 with antibodies to CD8 or MHC class I ligands has been found to induce apoptosis among immature CD4$^+$ CD8$^+$ thymocytes but not mature CD8$^+$ T cells (16), and this does not appear to be altered by loss of ST3Gal-I (22). Interestingly, de novo synthesis of CD45 after CD8$^+$ T-cell activation can account for the majority of increased PNA ligands (1), and CD45 has been found to participate in apoptosis (43, 46); however, our studies indicate that antibodies to CD45 are unable to induce or modulate PNA-induced apoptosis (data not shown) (48).

The identification of the relevant glycoprotein(s) and apoptotic pathway(s) involved will be necessary to resolve how core 1 O-glycan sialylation inhibits CD8$^+$ T-cell apoptosis and may require a glycoproteomics approach that is increasingly able to characterize biologically relevant glycan structures on glycoproteins (9, 10, 37). The dysfunction of one or a few glycoproteins can be responsible for the emergence of major phenotypes among glycosyltransferase-deficient mice, and such studies have implied that protein and glycan determinants can collaborate in the production of endogenous ligands for mammalian lectins (18, 40, 41).

Here we have used an inside-out approach to investigate the apoptotic pathway in ST3Gal-I function by probing the effect of intracellular Bcl-2 levels and Bim deficiency. Remarkably, the ability of Bcl-2 to reduce the CD8$^+$ T-cell contraction

phase of an immune response to SEB in vivo was eliminated by ST3Gal-I deficiency, resulting in reduced numbers of peripheral CD8$^+$ T cells which were mostly annexin V$^+$. Bcl-2 transgene expression continued to increase cell viability among all cells in vitro, concurrent with reduced frequencies of CD8$^+$ T cells that were PNA$^+$ and annexin V$^+$ at the cell surface. Transgenic Bcl-2 expression did not, however, interfere with the production of unsialylated core 1 O-glycans postactivation; therefore, the ability of Bcl-2 to inhibit the contraction phase in the presence of unsialylated core 1 O-glycans may reflect augmented downstream TCR and IL-2 receptor signaling, reducing the onset and rate of the contraction phase. Consistent with this interpretation, CD8$^+$ T-cell accumulation fails to occur in Bcl-2 transgenic mice, wherein normal peripheral levels of CD8$^+$ T cells exist.

In contrast, the intermediate phenotype observed in Bim- and ST3Gal-I-deficient mice includes a reduction in the frequency of apoptotic CD8$^+$ T cells compared with ST3Gal-I deficiency alone and appears to reflect a balance between the hyperaccumulation of CD8$^+$ T cells due to Bim deficiency and the ongoing effect of ST3Gal-I-deficient apoptosis. This is consistent with the finding that Bim deficiency failed to reduce the efficacy of PNA treatment as a means to induce apoptotic cell death in vitro in the absence of ST3Gal-I. A similar result was seen with Bcl-2 transgenic CD8$^+$ T cells in vitro and may further reflect the reduction in antigen levels and immune signaling that occur upon isolated ex vivo T-cell culture. These findings suggest an endogenous apoptotic stimulus that is lacking in vitro and is mimicked by PNA binding.

We propose that an endogenous multivalent lectin induces CD8$^+$ T-cell apoptosis during the contraction phase of the immune response by cross-linking one or more cell surface O glycoproteins that are modified by unsialylated core 1 O-glycans following TCR activation (Fig. 10A). In this model, CD8$^+$ T-cell immune activation via TCR stimulation initiates formation of a default and extrinsic apoptotic pathway to cell death that operates when immune signaling wanes. In Bim deficiency, unlike with elevated Bcl-2 levels, the vast increase in CD8$^+$ T-cell numbers saturates lectin binding sites and thereby reduces peripheral T-cell numbers to a normal homeostatic level (Fig. 10B). Sialylation by ST3Gal-I normally protects naive and memory CD8$^+$ T cells from this apoptotic stimulus in compartments where the apoptotic lectin is present and capable of cross-linking unsialylated core 1 O-glycans. Reconstitution kinetics among lymphopenic RAG-1-deficient mice were consistent with the presence of an apoptosis-inducing lectin more highly expressed in lymph node compartments compared with the spleen and absent from blood circulation, a finding consistent with the presence of a CD8$^+$ T-cell contraction phase following SEB immunization in lymph nodes, but not in the spleens or blood of Bim- and ST3Gal-I-deficient mice. Previous studies found that the contraction of Bim-deficient CD8$^+$ T cells proceeded normally in the lymph nodes after herpes simplex virus infection and occurred to a greater degree in the lymph nodes than in the spleen in the case of SEB (21, 45). The identity this putative apoptosis-inducing lectin is not yet known, although candidates include the β-galactosidase-binding mammalian galectins, several of which have been reported to induce apoptosis in T cells (13, 23, 25, 46, 58).

The homeostasis of CD8$^+$ T cells may be critically dependent on the presence or absence of multiple factors. Nevertheless, we have found that a specific alteration in protein O glycosylation during late stages of TCR stimulation and manifested on the cell surface by a posttranscriptional mechanism regulating ST3Gal-I function can play a dominant role in the CD8$^+$ T-cell contraction phase of the immune response by linking extracellular glycoprotein structure with molecular interactions that lead to apoptotic signal formation. Further resolving this process will elucidate a molecular pathway from the cell surface by which apoptotic signal formation controls peripheral CD8$^+$ T-cell homeostasis. The ability to modulate CD8$^+$ T-cell numbers by altering ST3Gal-I activity may be useful in reducing cytotoxic T-cell activity in tissue transplantation and attenuating pathogenesis in diseases such as glomerulonephritis and diabetes.

REFERENCES

1. **Amado, M., Q. Yan, E. M. Comelli, B. E. Collins, and J. C. Paulson.** 2004. Peanut agglutinin high phenotype of activated CD8$^+$ T cells results from de novo synthesis of CD45 glycans. J. Biol. Chem. **279:**36689–36697.
2. **Badovinac, V. P., A. R. Tvinnereim, and J. T. Harty.** 2000. Regulation of antigen-specific CD8$^+$ T cell homeostasis by perforin and interferon-γ. Science **290:**1354–1357.
3. **Badovinac, V. P., B. B. Porter, and J. T. Harty.** 2004. CD8$^+$ T cell contraction is controlled by early inflammation. Nat. Immunol. **5:**809–817.
4. **Bartholdy, C., J. P. Christensen, D. Wodarz, and A. R. Thomsen.** 2000. Persistent virus infection despite chronic cytotoxic T-lymphocyte activation in gamma interferon-deficient mice infected with lymphocytic choriomeningitis virus. J. Virol. **74:**10304–10311.
5. **Bouillet, P., D. Metcalf, D. C. S. Huang, D. M. Tarlington, T. W. H. Kay, F. Köntgen, J. M. Adams, and A. Strasser.** 1999. Proapoptotic Bcl-2 relative Bim required for certain apoptotic responses, leukocyte homeostasis, and to preclude autoimmunity. Science **286:**1735–1738.
6. **Brown, T. J., W. W. Shuford, W.-C. Wang, S. G. Nadler, T. S. Bailey, H. Marquhardt, and R. S. Mittler.** 1996. Characterization of a CD43/leukosialin-mediated pathway for inducing apoptosis in human T-lymphoblastoid cells. J. Biol. Chem. **271:**27686–27695.
7. **Carlow, D. A., S. Y. Corbel, and H. J. Ziltener.** 2001. Absence of CD43 fails to alter T cell development and responsiveness. J. Immunol. **166:**256–261.
8. **Casabo, L. G., C. Mamalaki, D. Kioussis, and R. Zamoyska.** 1994. T cell activation results in the physical modification of the mouse CD8b chain. J. Immunol. **152:**397–404.
9. **Chui, D., G. Sellakumar, R. S. Green, M. Sutton-Smith, T. McQuistan, K. W. Marek, H. R. Morris, A. Dell, and J. D. Marth.** 2001. Genetic remodeling of protein glycosylation *in vivo* induces autoimmune disease. Proc. Natl. Acad. Sci. USA **98:**1142–1147.
10. **Dell, A., and H. R. Morris.** 2001. Glycoprotein structure determination by mass spectrometry. Science **291:**2351–2356.
11. **Devadas, S., J. Das, C. Liu, L. Zhang, A. I. Roberts, Z. Pan, P. A. Moore, G. Das, and Y. Shi.** 2006. Granzyme B is critical for T cell receptor-induced cell death of type 2 helper T cells. Immunity **25:**237–247.
12. **Ellies, L. G., S. Tsuboi, B. Petryniak, J. B. Lowe, M. Fukuda, and J. D. Marth.** 1998. Core 2 oligosaccharide biosythesis distinguishes between selectin ligands essential for leukocyte homing and inflammation. Immunity **9:**881–890.
13. **Fukumori, T., Y. Takenaka, T. Yoshii, H. R. Kim, V. Hogan, H. Inohara, S. Kagawa, and A. Raz.** 2003. CD29 and CD7 mediate galectin-3-induced type II T-cell apoptosis. Cancer Res. **63:**8302–8311.
14. **Galvan, M., K. Murali-Krishna, L. L. Ming, L. Baum, and R. Ahmed.** 1998. Alterations in cell surface carbohydrates on T cells from virally infected mice can distinguish effector / memory CD8$^+$ T cells from naive cells. J. Immunol. **161:**641–648.
15. **Goldrath, A. W., and M. J. Bevan.** 1999. Selecting and maintaining a diverse T-cell repertoire. Nature **402:**255–262.
16. **Grebe, K. M., R. L. Clarke, and T. A. Potter.** 2004. Ligation of CD8 leads to apoptosis of thymocytes that have not undergone positive selection. Proc. Natl. Acad. Sci. USA **101:**10410–10415.

17. **Green, D. R.** 2005. Apoptotic pathways: ten minutes to dead. Cell **121:**671–674.

18. **Han, S., B. E. Collins, P. Bengston, and J. C. Paulson.** 2005. Homomultimeric complexes of CD22 in B cells revealed by protein-glycan cross-linking. Nat. Chem. Biol. **1:**93–97.

19. **Haring, J. S., V. P. Badovinac, and J. T. Harty.** 2006. Inflaming the CD8+ T cell response. Immunity **25:**19–29.

20. **Hildeman, D. A., T. Mitchell, T. K. Teague, P. Henson, B. J. Day, J. Kappler, and P. C. Marrack.** 1999. Reactive oxygen species regulate activation-induced T cell apoptosis. Immunity **10:**735–744.

21. **Hildeman, D. A., Y. Zhu, T. C. Mitchell, P. Bouillet, A. Strasser, J. Kappler, and P. Marrack.** 2002. Activated T cell death in vivo mediated by proapoptotic Bcl-2 family member Bim. Immunity **16:**759–767.

22. **Kao, C., M. M. Sandau, M. A. Daniels, and S. C. Jameson.** 2006. The sialyltransferase ST3Gal-I is not required for regulation of CD8-class I MHC binding during T cell development. J. Immunol. **176:**7421–7430.

23. **Kashio, Y., K. Nakamura, M. J. Abedin, M. Seki, N. Nishi, N. Yoshida, T. Nakamura, and M. Hirashima.** 2003. Galectin-9 induces apoptosis through the calcium-calpain-caspase-1 pathway. J. Immunol. **170:**3631–3636.

24. **Kitagawa, H., and J. C. Paulson.** 1994. Differential expression of five sialyltransferase genes in human tissues. J. Biol. Chem. **269:**17872–17878.

25. **Kuwabara, I., Y. Kuwabara, R. Y. Yang, M. Schuler, D. R. Green, B. L. Zuraw, D. K. Hsu, and F. T. Liu.** 2002. Galectin-7 (PIG1) exhibits proapoptotic function through JNK activation and mitochondrial cytochrome c release. J. Biol. Chem. **277:**3487–3497.

26. **Landolfi, N. F., J. Leone, J. E. Womack, and R. G. Cook.** 1985. Activation of T lymphocytes results in an increase in H-2-encoded neuraminidase. Immunogenetics **22:**159–167.

27. **Lau, L. L., B. D. Jamieson, T. Somasundaram, and R. Ahmed.** 1994. Cytotoxic T-cell memory without antigen. Nature **369:**648–652.

28. **Lenardo, M., K. M. Chan, F. Hornung, H. McFarland, R. Siegel, J. Wang, and L. Zheng.** 1999. Mature T lymphocyte apoptosis—immune regulation in a dynamic and unpredictable antigenic environment. Annu. Rev. Immunol. **17:**221–253.

29. **Liu, Y., R. Wada, H. Kawai, K. Sango, C. Deng, T. Tai, M. P. McDonald, K. Araujo, J. N. Crawley, U. Bierfreund, K. Sandhoff, K. Suzuki, and R. L. Proia.** 1999. A genetic model of substrate deprivation therapy for a glycosphingolipid storage disorder. J. Clin. Investig. **103:**497–505.

30. **Lohman, B. L., E. S. Razvi, and R. M. Welsh.** 1996. T-lymphocyte downregulation after acute viral infection is not dependent on CD95 (Fas) receptor-ligand interactions. J. Virol. **70:**8199–8203.

31. **Lohman, B. L., and R. M. Welsh.** 1998. Apoptotic regulation of T cells and absence of immune deficiency in virus-infected IFN-gamma receptor knockout mice. J. Virol. **72:**7815–7821.

32. **Manjunath, N., M. Correa, M. Ardman, and B. Ardman.** 1995. Negative regulation of T-cell adhesion and activation by CD43. Nature **377:**535–538.

33. **Marrack, P., and J. Kappler.** 2004. Control of T cell viability. Annu. Rev. Immunol. **22:**765–787.

34. **Matloubian, M., M. Suresh, A. Glass, M. Galvan, K. Chow, J. K. Whitmire, C. M. Walsh, W. R. Clark, and R. Ahmed.** 1999. A role for perforin in downregulating T-cell responses during chronic viral infection. J. Virol. **73:**2527–2536.

35. **Mombaerts, P., J. Iacomini, R. S. Johnson, K. Herrup, S. Tonegawa, and V. E. Papaioannou.** 1992. RAG-1-deficient mice have no mature B and T lymphocytes. Cell **68:**869–877.

36. **Moody, A. M., D. Chui, P. A. Reche, J. J. Priatel, J. D. Marth, and E. L. Reinherz.** 2001. Developmentally regulated glycosylation of the CD8αβ coreceptor stalk modulates ligand binding. Cell **107:**501–512.

37. **Moody, A. M., S. J. North, B. Reinhold, S. J. Van Dyken, M. E. Rogers, M. Panico, A. Dell, H. R. Morris, J. D. Marth, and E. L. Reinherz.** 2003. Sialic capping of CD8β core-1-O glycans controls thymocyte-major histocompatibility complex class I interaction. J. Biol. Chem. **278:**7240–7246.

38. **Murali-Krishna, K., J. D. Altman, M. Suresh, D. J. Sourdive, A. J. Zajac, J. D. Miller, J. Slansky, and R. Ahmed.** 1998. Counting antigen-specific CD8 T cells: a reevalulation of bystander activation during viral infection. Immunity **8:**177–187.

39. **Nguyen, L. T., K. McKall-Faienza, A. Zakarian, D. E. Speiser, T. W. Mak, and P. S. Ohashi.** 2000. TNF receptor 1 (TNFR1) and CD95 are not required for T cell deletion after virus infection but contribute to peptide-induced deletion under limited conditions. Eur. J. Immunol. **30:**683–688.

40. **Ohtsubo, K., S. Takamatsu, M. T. Minowa, A. Yoshida, M. Takeuchi, and J. D. Marth.** 2005. Dietary and genetic control of glucose transporter 2 glycosylation promotes insulin secretion in suppressing diabetes. Cell **123:**1307–1321.

41. **Ohtsubo, K., and J. D. Marth.** 2006. Glycosylation in cellular mechanisms of health and disease. Cell **126:**855–867.

42. **Onami, T. M., L. E. Harrington, M. A. Williams, M. Galvan, C. P. Larsen, T. C. Pearson, N. Manjunath, L. G. Baum, B. D. Pearce, and R. Ahmed.** 2002. Dynamic regulation of T cell immunity by CD43. J. Immunol. **168:**6022–6031.

43. **Ong, C. J., D. Chui, H. S. Teh, and J. D. Marth.** 1994. Thymic CD45 tyrosine phosphatase regulates apoptosis and MHC-restricted negative selection. J. Immunol. **152:**3793–3805.

44. **Ou, R., S. Zhou, L. Huang, and D. Moskophidis.** 2001. Critical role for alpha/beta and gamma interferons in persistence of lymphocytic choriomeningitis virus by clonal exhaustion of cytotoxic T cells. J. Virol. **75:**8407–8423.

45. **Pellegrini, M., G. Belz, P. Bouillet, and A. Strasser.** 2003. Shutdown of an acute T cell immune response to viral infection is mediated by the proapoptotic Bcl-2 homology 3-only protein Bim. Proc. Natl. Acad. Sci. USA **100:**14175–14180.

46. **Perillo, N. L., K. E. Pace, J. J. Seilhamer, and L. G. Baum.** 1995. Apoptosis of T cells mediated by galectin-1. Nature **378:**736–739.

47. **Piller, F., V. Piller, R. I. Fox, and M. Fukuda.** 1988. Human T-lymphcyte activation is associated with changes in O-glycan biosynthesis. J. Biol. Chem. **263:**15146–15150.

48. **Priatel, J. J., D. Chui, N. Hiraoka, C. J. Simmons, K. B. Richardson, D. M. Page, M. Fukuda, N. M. Varki, and J. D. Marth.** 2000. The ST3Gal-I sialyltransferase controls CD8+ T lymphocyte homeostasis by modulating O-glycan biosynthesis. Immunity **12:**273–283.

49. **Razvi, E. S., Z. Jiang, B. A. Woda, and R. M. Welsh.** 1995. Lymphocyte apoptosis during the silencing of the immune response to acute viral infections in normal, lpr, and Bcl-2-transgenic mice. Am. J. Pathol. **147:**79–91.

50. **Reich, A., H. Körner, J. D. Sedgwick, and H. Pircher.** 2000. Immune downregulation and peripheral deletion of CD8 T cells does not require TNF receptor-ligand interactions nor CD95 (Fas, APO-1). Eur. J. Immunol. **30:**678–682.

51. **Schachter, H., and I. Brockhausen.** 1989. The biosynthesis of branched O-glycans. Symp. Soc. Exp. Biol. **43:**1–26.

52. **Seder, R. A., and R. Ahmed.** 2003. Similarities and differences in CD4+ and CD8+ effector and memory T cell generation. Nat. Immunol. **4:**835–842.

53. **Sharma, V., M. Delgado, and D. Ganea.** 2006. Granzyme B, a new player in activation-induced cell death, is down-regulated by vasoactive intestinal peptide in Th2 but not Th1 effectors. J. Immunol. **176:**97–110.

54. **Siegel, R. M., F. K. Chan, H. J. Chun, and M. J. Lenardo.** 2000. The multifaceted role of Fas signaling in immune cell homeostasis and autoimmunity. Nat. Immunol. **1:**469–474.

55. **Snapp, K. R., C. E. Heitzig, L. G. Ellies, J. D. Marth, and G. S. Kansas.** 2001. Differential requirements for the O-linked branching enzyme core 2 β 1-6-N-glycosaminyltransferase in biosynthesis of ligands for E-selectin and P-selectin. Blood **97:**3806–3811.

56. **Strasser, A., A. W. Harris, and S. Cory.** 1991. Bcl-2 transgene inhibits T cell death and perturbs thymic self-censorship. Cell **67:**889–899.

57. **Strasser, A.** 2005. The role of BH3-only proteins in the immune system. Nat. Rev. Immunol. **5:**189–200.

58. **Sturm, A., M. Lensch, S. Andre, H. Kaltner, B. Wiedenmann, S. Rosewicz, A. U. Dignass, and H. J. Gabius.** 2004. Human galectin-2: novel inducer of T cell apoptosis with distinct profile of caspase activation. J. Immunol. **173:**3825–3837.

59. **Taira, S., and H. Nariuchi.** 1988. Possible role of neuraminidase in activated T cells in the recognition of allogeneic Ia. J. Immunol. **141:**440–446.

60. **Wang, X. Z., S. E. Stepp, M. A. Brehm, H. D. Chen, L. K. Selin, and R. M. Welsh.** 2003. Virus-specific CD8 T cells in peripheral tissues are more resistant to apoptosis than those in lymphoid organs. Immunity **18:**631–642.

61. **Wu, W., P. H. Harley, J. A. Punt, S. O. Sharrow, and K. P. Kearse.** 1996. Identification of CD8 as a peanut agglutinin (PNA) receptor molecule on immature thymocytes. J. Exp. Med. **184:**759–764.

62. **Zhang, M., S. M. Park, Y. Wang, R. Shah, N. Liu, A. E. Murmann, C. R. Wang, M. E. Peter, and P. G. Ashton-Rickardt.** 2006. Serine protease inhibitor 6 protects cytotoxic T cells from self-inflicted injury by ensuring the integrity of cytotoxic granules. Immunity **24:**451–461.

63. **Zhou, S., R. Ou, L. Huang, and D. Moskophidis.** 2002. Critical role for perforin-, Fas/FasL-, and TNFR1-mediated cytotoxic pathways in downregulation of antigen-specific T cells during persistent viral infection. J. Virol. **76:**829–840.

64. **Zhumabekov, T., P. Corbella, M. Tolaini, and D. Kioussis.** 1995. Improved version of a human CD2 minigene based vector for T cell-specific expression in transgenic mice. J. Immunol. Methods **185:**133–140.